Super-heavy element research

2015 Rep. Prog. Phys. 78 036301

(http://iopscience.iop.org/0034-4885/78/3/036301)

IOP Publishing Reports on Progress in Physics
Rep. Prog. Phys. **78** (2015) 036301 (22pp) doi:10.1088/0034-4885/78/3/036301

Review Article

Super-heavy element research

Yu Ts Oganessian and V K Utyonkov

Joint Institute for Nuclear Research (JINR), Joliot-Curie 6, RU-141980 Dubna, Russian Federation

E-mail: oganessian@jinr.ru

Received 24 July 2014, revised 10 November 2014
Accepted for publication 27 November 2014
Published 9 March 2015

Invited by Robert Tribble

Abstract

A review of the discovery and investigation of the 'island of stability' of super-heavy nuclei at the separator DGFRS (FLNR, JINR) in the fusion reactions of ^{48}Ca projectiles with target nuclei ^{238}U-^{249}Cf is presented. The synthesis of the heaviest nuclei, their decay properties, and methods of identification are discussed. The role of shell effects in the stability of super-heavy nuclei is demonstrated by comparison of the experimental data and results of theoretical calculations. The radioactive properties of the new nuclei, the isotopes of elements 112–118 as well as of their decay products, give evidence of the significant increase of the stability of the heavy nuclei with rise of their neutron number and approaching magic number $N = 184$.

Keywords: super-heavy elements, alpha decay, spontaneous fission

1. Introduction

The limits of nuclear stability, as it is known, are determined by interaction of nucleons in the nucleus. The neutron excess in nuclei leads to a decrease in the neutron separation energy. The limit comes at $B_n = 0$ MeV (the neutron drip line). Similarly, $B_p = 0$ MeV (the proton drip line) determines the limit of existence of proton-rich nuclei. Another limitation arises for the extreme nuclear mass, which is defined by the probability of spontaneous fission (SF). In fact, when the fission barrier vanishes ($B_f = 0$ MeV), the nucleus loses its stability against fission ($T_{SF} \sim 10^{-19}$ s). In the macroscopic approach (e.g. the liquid-drop model) the limit of existence of nuclei appears practically immediately after $Z \approx 100$ [1]. At the same time, it has been observed that in the binding energy of nuclei in their ground and highly deformed states there are variations depending on the proton or neutron number (nuclear shells). Also, the macroscopic models could not explain the variations of the fission barriers of the heavy nuclei: two times higher barrier in ^{208}Pb ($B_f \approx 27$ MeV), practically unchanged fission barrier heights in the isotopes of the actinides from U to Fm and the nuclear shape isomerism [2], which manifests itself in heavy nuclei as 35 SF isomers [3] and many other effects, which have been seen in various experiments (figure 1). It had become obvious that the macroscopic approaches needed some corrections caused by structure of individual nucleus. The main achievements of the microscopic theory are connected with the development of the method of calculating such corrections for the ground and highly deformed states [9] based on the Nilsson or Woods–Saxon single particle potential to the smooth, macroscopic part of the energy.

The main structure corrections are governed by the nuclear shell effect. The concept of nuclear shells is here defined as a large-scale non-uniformity in the energy distribution of the individual particle states near the Fermi energy [10] directly connected to the nuclear binding energy. In many publications (e.g. see the reviews [10–13] and references therein), a number of the existing disagreements with experiment were explained by taking into account the shell effect when calculating the nuclear energy. One important consequence of these calculations was the disclosure of a significant gap in the spectrum of low lying levels in the region of the hypothetical super-heavy nuclei (SHN), viz. of a new (following $N = 126$) closed spherical neutron shell at $N = 184$ [14–17].

It was also shown that the considerable variations in the binding energy of spherical nuclei were due to the nuclear shells and that shell effects might be present also in deformed 'magic nuclei' (deformed shells) [9, 10, 18]. And finally, at further and quite significant increase of the deformation

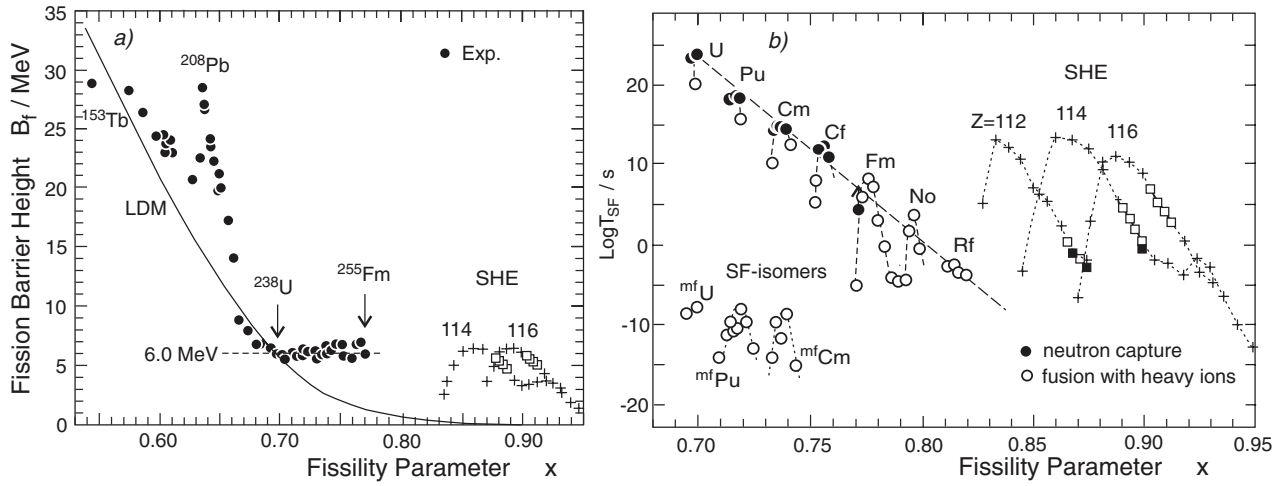

Figure 1. (*a*) Fission barrier heights as a function of the fissility parameter $x = (Z^2/A)/(Z^2/A)_{crit}$ at $(Z^2/A)_{crit} = 50.883$ [4]. Black points show experimental data, solid line—calculations in the liquid drop model [5, 6], crosses—calculated fission barrier heights in the macroscopic–microscopic model [7, 8] for the isotopes of elements 114 and 116, open squares—the same for the nuclei produced in the ^{242,244}Pu, ^{245,248}Cm + ^{48}Ca reactions. (*b*) Half-lives with respect to SF as a function of the fissility parameter *x*. Black points and open circles denote experimental values T_{SF}(exp) for SF of even–even nuclei from the ground and isomeric states. Dashed line is drawn to guide the eye though the maximum T_{SF}(exp) values and is extrapolated into the transactinide region according to macroscopic concept. Crosses show calculated values T_{SF}(th) in the macroscopic–microscopic model [7, 8] for even–even isotopes of elements 112, 114 and 116, open squares—the same for the nuclei produced in the ^{242,244}Pu, ^{245,248}Cm + ^{48}Ca reactions, black squares—the same for the isotopes for which the SF half-lives have been measured.

arising in fission, *the shell effects continued to play an important role* in defining the potential energy and the nuclear inertial masses [7, 10].

The predictions of the nuclear properties change significantly depending on the effect of the new shells. The sum of the smooth part of the deformation energy E_d(LD) and the shell correction ΔE_d(Shell) bring forth the appearance of a fission barrier.

For the heaviest nuclei with Z = 112–114 and N = 180–184 (see figure 2), the fission barrier height may amount to $B_f > 6$ MeV (higher than for ^{238}U). Therefore, the partial SF half-lives, as shown in the calculations of [7, 8], increase up to ~10^5 year (figure1(*b*)). Then, T_{SF} exceeds the estimates of the macroscopic models by a factor of 10^{30}! Less striking, but also quite strong, is the effect expected for deformed nuclei with Z = 106–108 and $N \approx 162$, the effect of the deformed shells suppresses the probability of SF by a factor of $>10^{20}$. Here, an interesting situation arises.

Because of the high stability with respect to SF, the heaviest nuclei will undergo α- or β-decay (T_α, $T_\beta << T_{SF}$). From the calculated partial half-lives T_α, $T_{EC,\beta}$ and T_{SF}, shown in figure 3, we may get an impression of the scenarios and the decay properties of the heaviest nuclei depending on Z and N. The consecutive α decays will follow until the shell effect weakens and SF becomes the main decay mode. In the region of $N < 162$ this is observed for even–even isotopes [20]. In the case of odd nuclei, due to the large hindrances to SF, α decay may occur down to long-living nuclei without competition from SF. In fact, this is observed in the experiments with Pb-target based reactions [20, 21]. For the heavier neutron-rich nuclei, the decay sequences of both even and odd isotopes will end by SF. The total decay time will be then determined to a great extent by the neutron number of the parent nucleus.

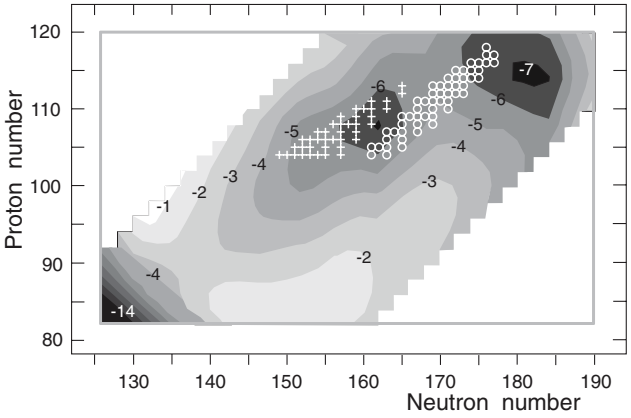

Figure 2. The map of the shell corrections ΔE_{shell} to the nuclear macroscopic potential energy [18, 19]. The numbers at the contour curves correspond to the amplitude of the shell correction (in MeV). Crosses denote nuclei with $Z \geq 104$, obtained in cold-fusion reactions, open circles—in actinides (Act) + ^{48}Ca reactions.

When approaching the N = 184 shell, we may expect a strong increase in the decay time.

Above we gave an example of the predictions of the macroscopic–microscopic models (MM). Other, purely microscopic self-consistent approaches as the Hartree–Fock–Bogoliubov (HFB) model and the relativistic mean field (RMF) theory also predict significant increase of the binding energy of heavy nuclei at N = 162 and N = 184. In spite of differences in these models, the maximum shell effect corresponds to N = 184 (like in MM calculations) but the proton shell closure with a higher number of protons Z = 120, 122, 124 or even 126 is expected (see review [22] and references therein). Meantime, uncertainties in the quantitative estimations of the

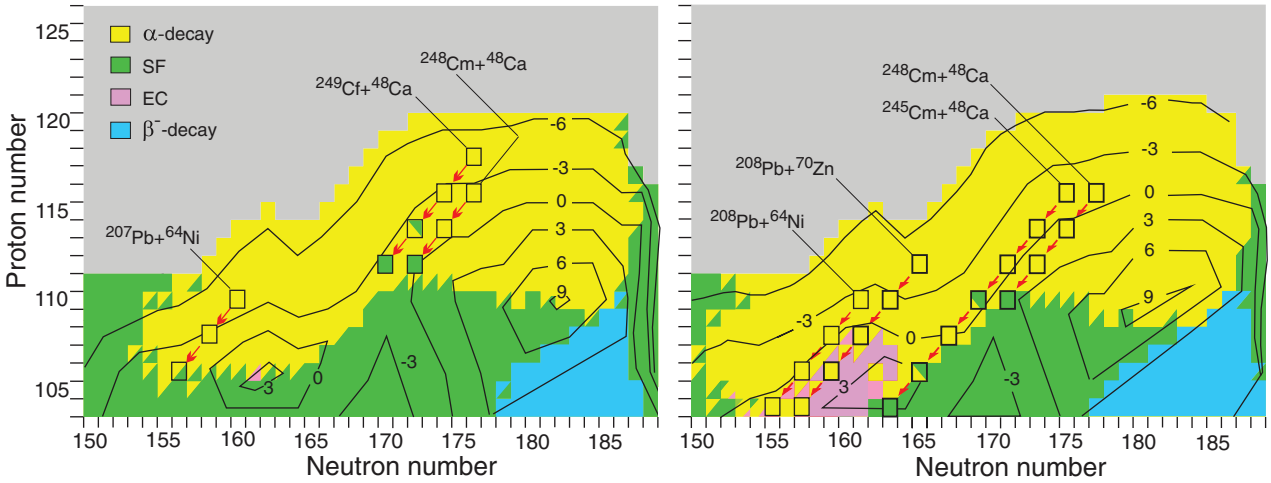

Figure 3. Contour map of the calculated half-lives as Log($T_{1/2}$) (in seconds) and decay modes of the nuclei with $Z \geq 104$ and $N \geq 150$ (taken from [20]). The left graph refers to even–even nuclei, the right one—to odd-A nuclei. The regions corresponding to different decay modes are shown in different color. The consecutive decay of nuclei, produced in cold fusion and in actinides + ^{48}Ca reactions are also shown (see text for details).

nuclear shell effects do not change the general conclusion of the theory that in the large interval of masses from 250 to 320 'islands of stability' may arise, considerably changing the limits of existence of atomic nuclei.

2. Reactions of synthesis of super-heavy nuclei

As it was shown in various experiments, the methods of consecutive neutron capture previously used for production of nuclei with $Z \leq 100$ or transfer reactions of nuclei, even so heavy as U + U, cannot be applied for synthesizing super-heavy elements[1]. The only way for producing the heaviest nuclei remains making use of complete-fusion reactions which were applied for the synthesis of elements of the second hundred.

In theory, the process of formation of the evaporation residue (ER) consists of three consecutive stages. At the first stage, colliding nuclei overcome the Coulomb barrier and approach the point of contact. Quasi-elastic and deep-inelastic reaction channels dominate at this stage, leading to formation of projectile-like and target-like fragments in the exit channel. Then, the composite system can evolve into the configuration of an almost spherical compound nucleus (CN). After dynamical deformation and exchange by nucleons, two touching nuclei can re-separate into fragments similar to colliding nuclei or can go directly to fission channels without formation of spherical compound nucleus which is called quasi-fission. Finally, the compound nucleus cools down by the emission of neutrons and γ rays surviving fission and forming ER in its ground state. This process takes place in strong competition with fission of excited nucleus.

For each angular momentum l the partial ER cross section $\sigma_{xn}(E^*, l)$ for production of the final nucleus in its ground state at projectile energy E and corresponding excitation energy E^* of CN is factorized as the product of the partial capture cross section $\sigma_{\text{capt}}(E, l)$, the fusion probability $P_{\text{fus}}(E, l)$ and the survival probability $P_{\text{surv}}(E^*, l)$,

$$\sigma_{xn}(E^*, l) = \sigma_{\text{capt}}(E, l) \cdot P_{\text{fus}}(E, l) \cdot P_{\text{surv}}(E^*, l) . \quad (1)$$

The difference in mass of the initial nuclei A_P, A_T and the final nucleus $A_{CN} = A_P + A_T$ defines the excitation energy of the CN E^*. The minimum value of E^* at the reaction Coulomb barrier B_C is:

$$E^*_{\text{min}} = B_C - Q \text{ with } Q = M_{CN} - (M_P + M_T) . \quad (2)$$

Energy E^*_{min} depends on the masses (in eV) of the interacting nuclei. When the mass ratio A_P/A_T increases (from $A_P = 4$ to 20–30), with fixed Z_{CN}, the excitation energy increases also (rise of the Coulomb barrier), but then becomes lower due to increasing Q. The advance to the nuclei with closed proton or neutron shells leads to an additional reduction of E^*_{min} [23].

Since 1974, the cold fusion reactions of ^{208}Pb, ^{209}Bi with massive projectiles ($A_P \geq 50$) have been used in the synthesis of the heaviest elements. With practically fixed mass of the target (^{208}Pb or ^{209}Bi), the rise of the atomic and mass numbers of the evaporation products is entirely connected with the increase in the mass (and charge) of the projectile. When the projectile becomes more and more heavy, the excitation energy of the CN decreases down to $E^* \approx 15$–10 MeV (cold fusion). Transition to the ground state takes place by the emission of only one neutron [20, 21]. As a result, the survivability of the CN $P_{xn}(E^*)$ significantly increases, this being the main advantage of cold-fusion reactions.

In cold-fusion reactions, ERs are some 10–15 mass units shifted from the β-stability line which leads to a considerable decrease in their half-lives. Furthermore, the cross section of ERs produced in cold-fusion reactions exponentially decreases with the increase of Z_{CN} because of rise of the Coulomb repulsion forces. When Z_{CN} changes from 102 to 113, the cross section decreases by a factor of 10^8. Because of small neutron excess in the evaporation products and further considerable decrease of the cross section with increase of the projectile mass ($A_P > 70$), it is impossible to reach the region

[1] In this paper, we will use term 'super-heavy elements' for the heaviest nuclei (atoms) which stability is governed by existence of the new spherical shells at $Z = 114$ and $N = 184$ predicted for the first time within the macroscopic–microscopic nuclear theory.

of SHN. Obviously, for the synthesis of these nuclei ($Z \geq 114$) with high neutron excess, it was necessary to look for other reactions.

In order to decrease the factors hindering fusion, it is desirable to make use of more asymmetric reactions and to obtain an increase in the neutron number of the ERs by using both target and projectile nuclei with maximum neutron excess. As a target material, it is reasonable to use neutron-rich isotopes of the actinides produced in high-flux reactors and thus have the largest neutron excess. Among the projectiles, the undoubted advantage is possessed by the doubly magic nucleus of the rare isotope ^{48}Ca. The CN ^{292}114, produced, for example, in the fusion of ^{244}Pu and ^{48}Ca ($Z_P \cdot Z_T = 1880$), acquires 8 additional neutrons compared to the problematic ^{208}Pb + ^{76}Ge ($Z_P \cdot Z_T = 2624$) reaction. Coulomb repulsion in the reaction ^{244}Pu + ^{48}Ca decreases by almost 40%, which in turn should lead to a strong decrease in the factors hindering the formation of the CN.

The last stage—the survival of the CN—is the decisive one in the given method of synthesis of the heaviest nuclei. The estimations of $E^*_{\min}$ and experiments aimed towards measuring the excitation functions for evaporation products, have shown that the CN with $Z_{CN} = 112$–118, when formed in actinides + ^{48}Ca reactions, may attain excitation energy from 30 to 55 MeV (see section 4). This energy will be released by a cascade emission of 2 to 5 neutrons (the evaporation of charged particles is significantly less probable) and γ-rays. At each step, neutron evaporation and fission compete strongly. The survival probability can be expressed simply as:

$$P_{xn}(E^*) \sim \prod_{i=1}^{x} (\Gamma_n / \Gamma_f)_i \sim \prod_{i=1}^{x} \exp[(B_f - B_n / T)]_i., \quad (3)$$

where B_f and B_n are the fission barrier height and the binding energy of the neutron, respectively, T is the temperature of the CN and x—the number of emitted neutrons.

According to calculations, the fission-barrier height of nuclei with $Z > 104$ is entirely determined by the amplitude of shell correction. The large decrease of production cross sections for increasingly heavy nuclei, observed in asymmetrical hot-fusion reactions, is connected with their lower survivability caused by reduce of fission barriers for CN with an increase in Z and N. However, if the predictions of the theoretical models about the existence of the next closed shell $N = 184$ are justified, the fission barrier height will again increase when advancing the region where $N_{CN} \geq 174$ and $Z_{CN} \geq 112$. In turn, the nuclear survivability will increase too and as a result, one can expect even *a rise in the cross section* for heavy nuclei with higher Z and large neutron excess.

3. Experiments

The half-lives of nuclei, products of the complete-fusion reactions of neutron-rich isotopes of heavy actinide elements with ^{48}Ca projectiles, were expected to vary in a wide range: from microseconds (for the even–even isotopes of the heavy elements, see, e.g. [7, 22]) up to days (for the products of sequential decay of the odd nuclei). Their calculated predominant

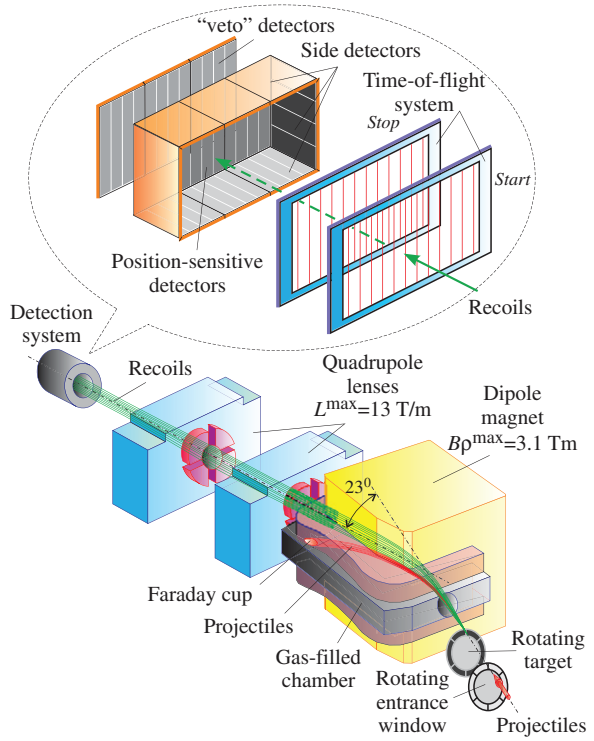

Figure 4. Layout of the DGFRS and detection system. L^{max} and $B\rho^{max}$ are maximum field gradient and magnetic rigidity, respectively.

decay modes were α decay and SF. Production cross sections of the ERs could be at the level of a picobarn (10^{-36} cm^2) or even lower. The recoiling nuclei, formed with full momentum transfer from the projectile to the CN, leave the target layer in the beam direction. Therefore, experimental equipment should separate them from the beam particles, scattered nuclei and transfer-reaction products.

The Dubna gas-filled recoil separator (DGFRS) is shown schematically in figure 4. The DGFRS has a DQ_hQ_v magnetic configuration: a flat-field dipole magnet with inclined poles for horizontal focusing (D) followed by horizontally (Q_h) and vertically (Q_v) focusing quadrupole magnets.

The ERs recoil out of a thin target with the momentum of the beam particle and enter the dipole-magnet chamber filled by gas at the pressure of about 1 Torr [24]. For keeping gas inside the DGFRS at the beam intensities of ^{48}Ca up to 10^{13}/s delivered by the U400 cyclotron, a rotating 1.6 μm Ti window is mounted at its entrance as well as a 0.5–1.5 μm Mylar fixed window separating the detection system. After emerging from the target layer, the heavy atoms have a large ion charge ($q \approx 20^+$) with broad distribution. Due to charge exchange in consecutive collisions with the gas atoms, the distribution of the ERs charges rapidly becomes narrower and the mean charge decreases to the equilibrium value ($q \approx 6^+$) [25] whereas average ion charge of projectiles is $q \approx 18^+$ due to their high velocity. In sequential collisions with the atoms of the medium, the heavy atoms slow down and move along some average trajectory. Ions with mass (m), average charge (q) and velocity (v), will be deflected in a magnetic field strength (B) following a trajectory with curvature radius (ρ). The ER trajectory in the field of a gas-filled

dipole magnet is determined by momentum and charge as follows:

$$B\rho = m\, v_0 Z^{-1/3} e^{-1} = 0.0227 A\, Z^{-1/3}\,[\mathrm{T\,m}]\,, \qquad (4)$$

where A is the mass number and v_0 is the velocity of the electron (e) in Bohr's hydrogen atom ($2.19 \times 10^6\,\mathrm{m\,s^{-1}}$).

Among all the reaction products, the complete-fusion reaction products have the largest possible mass. Accordingly, the other products—target-like or projectile-like ions—will be spatially separated in flight from the ERs following the trajectories with lower curvature radii. Thus, in experiments on the synthesis of SHN, the DGFRS suppresses the full-energy ^{48}Ca projectiles, projectile-like ions and target-like nuclei by factors of about 3×10^{15}–10^{17}, 3×10^{13}–6×10^{14} and 10^4–10^6, respectively [26, 27]. The transmission efficiency of the separator for Z = 112–118 nuclei was estimated to be about 35–40% [24] for the size of the focal-plane detector of $120 \times 40\,\mathrm{mm^2}$.

A specific characteristic of the DGFRS is the hydrogen gas used in the separator, which enables better suppression of projectile- and target-like recoils at the focal plane than the helium gas [28, 29] which is used in other separators (e.g. BGS [29, 30], TASCA [31, 32]). Due to the approximately linear dependence of the ion charge on velocity, transmission of ERs produced in the same reaction at different projectile energies varies weakly. Three isotopes of Fl (Z = 114) were observed in this reaction with masses 287, 288 and 289 which differ by only about 0.3%; the change of the DGFRS setting was not needed. After separation in the DGFRS dipole magnet from the beam particles and products of unwanted reactions, the ERs are focused by the quadrupole doublet (see figure 4) onto the separator focal plane located about 4 m downstream. The heaviest nuclei, leaving the target with energy of 35–40 MeV, pass over this distance in about 1 μs. Due to kinematics of ^{252}No close to that of the SHN produced in the ^{48}Ca-induced reactions, the ^{206}Pb(^{48}Ca,2n)^{252}No reaction can be used for testing and calibration of the separator and detection system. This reaction was used for determining the optimal thickness of the target also. The total yield of ^{252}No increases with growth of the target thickness up to approximately $0.5\,\mathrm{mg\,cm^{-2}}$. For thicker targets, the yield remains the same because of the lower transmission caused by multiple scattering of the recoils [33].

In the experiments on the synthesis of the heaviest nuclei performed at the DGFRS, targets of actinide oxides were used with thickness of about $0.4\,\mathrm{mg\,cm^{-2}}$ electrodeposited on a 1.6 μm Ti foil. Enriched isotopes of ^{238}U, ^{237}Np, ^{242,244}Pu, ^{243}Am, ^{245,248}Cm, ^{249}Bk and ^{249}Cf were used as target material. Each individual target had an area of 5.4–6.0 cm^2 in the shape of an arc segment with an angular extension of 60° and an average radius of 60 mm. The six segments were mounted on a disc that was rotated at 2000 rpm in plane perpendicular to the beam direction. The total area of the target was 32–36 cm^2, the total weight of the target material was about 10–15 mg. Before implantation into the detector, the separated ERs passed through a time-of-flight (TOF) measuring system that consists of two (start and stop) multiwire proportional chambers placed within 6.5 cm from each other and filled with pentane at ≈1.5 Torr. The TOF system allows distinguishing recoils coming from the separator and passing through the TOF system from signals, arising from α decay or SF of the implanted nuclei (without a TOF signal). In order to eliminate the background from the fast light charged particles (protons, α's, etc produced from direct reactions of projectiles with the DGFRS media) with signal amplitudes lower than the registration threshold of the TOF detector, a 'veto' silicon detector was placed behind the front detector (figure 4).

ERs are finally implanted in the focal-plane detector consisting of 12 vertical position-sensitive strips (three $4 \times 4\,\mathrm{cm^2}$ 0.3 mm-thick chips, each with four strips) providing horizontal resolution. The vertical position is determined by the resistive charge division within each strip. The implantation depth of ERs in the Si detector is lower by several times than α-particle range of SHN; thus, α particles can escape the focal-plane detector. To detect these particles as well as fission fragments, eight similar detectors without position sensitivity were located upstream and perpendicular to the focal-plane detector forming a five-sided box configuration. This results in increase of detection efficiency for full-energy α particles from about 52% for focal-plane detector only to approximately 87% after reconstruction of their energies deposited in the focal-plane and side detectors. The detection efficiency for SF of the implanted nuclei is close to 100%. Since 2012, to increase the position granularity of the detectors, which reduces the probability of observing sequences of random events that could imitate decay chains of synthesized nuclei, the new focal-plane detectors have been used. These consiste of two $6 \times 6\,\mathrm{cm^2}$ detectors each having 16 strips with position sensitivity and six similar side detectors without position sensitivity. The detection system of the DGFRS was calibrated by registering the recoil nuclei and decays (α or SF) of known isotopes of No and Th and their descendants produced in the reactions ^{206}Pb(^{48}Ca,2n) and $^{\mathrm{nat}}$Yb(^{48}Ca,3-5n), respectively. Using known energies of ^{215}Ra and ^{217}Th the energy resolutions (full width at half maximum (FWHM)) were determined separately for α particles completely absorbed in the focal-plane detector, for α particles that escaped this detector with a low energy release and were registered by a side detector and for α particles detected only by a side detector (without a focal-plane position signal). For instance, in a recent experiment with ^{249}Bk target [34] these values were 34–73 keV, 83–120 keV and 0.73–0.98 MeV, respectively. Fission fragments from the decay of ^{252}No implants produced in the ^{206}Pb + ^{48}Ca reaction were used for the total kinetic energy (TKE) calibration. The typical position resolutions of correlated ER-α and ER-SF signals were 1.1–1.8 and 0.5–1.2 mm [34], respectively. For α particles detected by both the focal-plane and side detectors, the ER-α position resolution depends on the energy deposited in the focal-plane detector and is generally inferior to that obtained for the full-energy signal.

From theoretical calculations and the available experimental data, one can estimate the expected α-particle energies of the ERs and their descendant nuclei that could be produced in a specific reaction of synthesis. For α particles emitted by the parent or daughter nuclei, it is possible to choose wide enough energy and time gates $\delta E_{\alpha 1}$, $\delta t_{\alpha 1}$, $\delta E_{\alpha 2}$, $\delta t_{\alpha 2}$, etc (accounting for

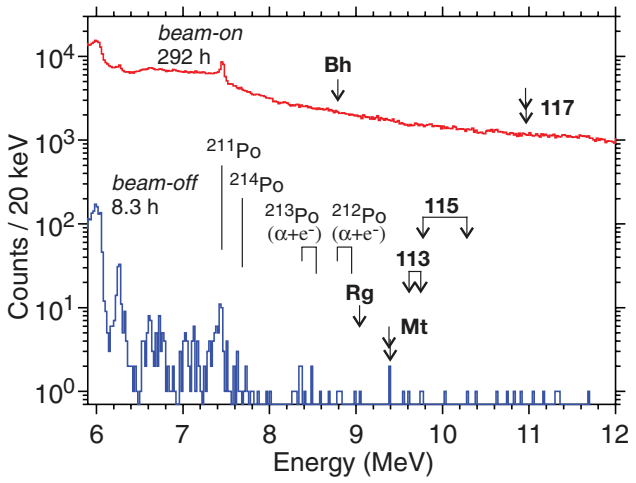

Figure 5. Total energy spectra of beam-on α-like signals (all events detected by the focal-plane detector or both the focal-plane and side detectors without registering TOF signal) and beam-off α particles recorded during the 247-MeV ^{249}Bk+^{48}Ca run. Durations of the beam-on and beam-off intervals are given. The arrows show the energies of events observed in two correlated decay chains of ^{294}117 [36].

all the uncertainties in the estimation of the expected energies and half-lives of the synthesized nuclei) and employ a special low-background detection scheme [35]. For instance, in [34] during the irradiation of the target, the beam was switched off after a recoil signal was detected with parameters of implantation energy and TOF expected for ERs, followed by an α-like signal within energy interval $\delta E_{\alpha 1} = 10.7$–$11.3$ MeV in the same strip within some position window (3.2 mm) and time interval $\delta t_{\alpha 1}$ (0.4 s). If the first α particle escaped the focal-plane detector and a position signal was not detected, then switching off the beam could be done when the second α particle in the corresponding $\delta E_{\alpha 2}$ (9.6–10.7 MeV) and $\delta t_{\alpha 2}$ (2 s) intervals was detected. If, during the first preset beam-off time interval, an α particle with energy expected for daughter nuclei was registered in any position of the same strip, the beam-off interval could be automatically extended to any time. This operating mode of the DGFRS is illustrated by detection of long decay chains of the odd–odd isotope of element 117 produced in the ^{249}Bk(^{48}Ca, $3n$)^{294}117 reaction [36]. Figure 5 shows the spectrum of α-like signals (all events detected by the focal-plane detector or both the focal-plane and side detectors without a registered TOF signal) in all strips accumulated during the 247 MeV ^{249}Bk + ^{48}Ca experiment. The α-particle spectrum detected during beam-off time intervals is also shown. In the high-energy part of the α-particle spectrum, where the decays of daughter nuclei ^{274}Bh to ^{290}115 (E_α = 8.5–10.5 MeV) are expected, 16 events were detected with average counting rate of about 2/h. This demonstrates very low random probability for detection of 7 α particles (shown by arrows) which belong to the decays of the daughter isotopes of ^{294}117 and occur within about a 3 min time interval after the decay of the parent nucleus. The calculated numbers of random sequences imitating each of the observed decay chains ranged from 2×10^{-4} to 3×10^{-20} depending on number of registered nuclei in the chain and counting rate of random events in the focal-plane and side detectors [34].

One of the crucial questions in the synthesis of SHN lies in identification of the new isotopes or experimental determination of their atomic (Z) and mass ($Z + N$) numbers. Note, all the decay chains of SHNs were terminated by SF of previously unknown nuclei. Moreover, these descendant neutron-rich nuclides with lower Z cannot be synthesized and identified in direct reactions because of lack of reactions with stable projectiles leading to these nuclei. That is why the method of genetic α-particle correlations between first observed and well-known nuclei, widely used during last decades (see, e.g. [20, 21]), can be applied after independent identification of one of the members of the decay chain.

At the same time, the super-heavy nuclei and their daughters can be identified by other methods [37]. One of these is connected with mechanism of the complete-fusion reaction which essentially differs from other reactions of ^{48}Ca projectiles with heavy target nuclei. The de-excitation of CN occurs via evaporation of neutrons; their number depends on the excitation energy. The shape of excitation functions $\sigma_{xn}(E^*)$ looks like assimetric pseudo–Gaussian curve with FWHM of about 10 MeV and with maximum located at the energy corresponding to the number of evaporated neutrons (see, e.g. figures 7 and 9 below). The probability of evaporation of charged particles (protons or α particles) is suppressed due to high Coulomb barrier in heavy CN. The DGFRS strongly separates forward-peaked ERs with huge suppression of the scattered beam particles and the products of incomplete fusion (like αxn) or transfer reactions.

The measurement of excitation function of the reaction allows determining the number of evaporated neutrons and thus, the masses of ERs when two or even three different isotopes are registered and difference of their decay properties is in agreement with expectations for the neighbouring isotopes of the same element. Practically all the investigated reactions which resulted in observation of SHN with Z = 112–118 at the DGFRS were studied at several bombarding energies [4, 26, 27, 34, 36].

An additional approach to the identification of nuclei is connected with variation of mass and charge of target in the cross bombardments with ^{48}Ca projectiles. In this method, one and the same nucleus can be observed either as the product of evaporation of a different number of neutrons from CN produced in the reactions with different target isotopes or as α-decay product of parent nuclide synthesized in the reaction with a heavier target nucleus (with higher Z). As an example, figure 6 shows cross reactions used in experiments on the synthesis of Fl and Lv. Finally, the α decay properties and SF half-lives of synthesized nuclei can evidently demonstrate their origin. For α decay of the even–even nuclei, one may expect with large probability transitions through ground states of the parent and daughter nuclei. In this case, measured α-particle energies E_α and partial half-lives T_α should reflect energy (Q_α) and probability of α transitions, which can be compared with predictions of different theoretical models of α decay and systematics of Q_α values for numerous known nuclei.

Comparison of α-particle energies of even-Z nuclei with those observed for neighbouring odd-Z nuclei can provide

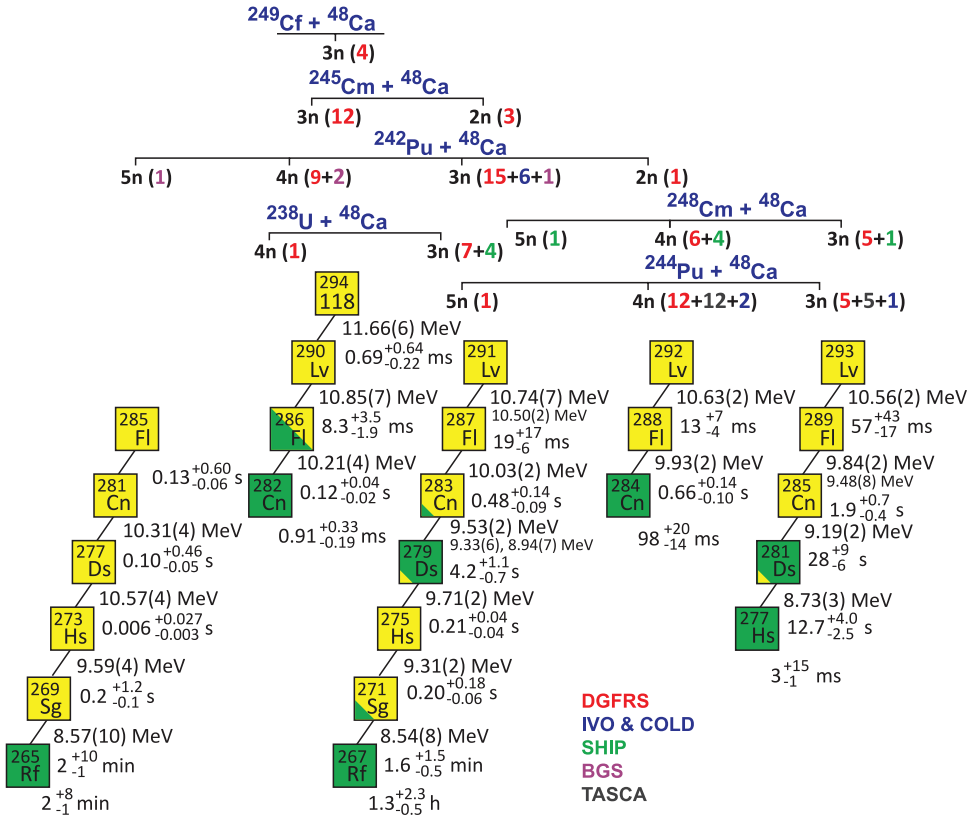

Figure 6. Summary decay properties of the isotopes of even-*Z* elements observed among the products of ^{48}Ca beam and ^{238}U, ^{242,244}Pu, ^{245,248}Cm and ^{249}Cf target reactions. The numbers of the decay chains of the given isotopes, the products of corresponding *xn*-evaporation channels, observed in experiments with use of the DGFRS (in red) [39–45], IVO setup with COLD detector (in blue) [46–49], SHIP (in green) [50, 51], BGS (in magenta) [52, 53] and TASCA (in grey) [32, 54] are shown. The average energies of α particles and half-lives are given for all α emitters observed in these experiments (yellow squares). The energies of rare α lines are given by smaller font. The energy uncertainties given in brackets correspond to the data with the best energy resolution. For spontaneously fissioning nuclei marked by green squares the half-lives are listed.

valuable information for identification. For unhindered α decays, from Geiger–Nuttall relation $T_\alpha(Z, Q_\alpha)$, one can estimate atomic numbers of all nuclei in the α-decay chains of the new elements. For SF nuclides, the half-lives of nuclei with an odd number of neutrons and/or protons exceed those for even–even nuclei by several orders of magnitude [38].

In approaching neutron shell $N = 184$, a considerable increase in the stability of SHN is expected. Super-heavy nuclei—neutron-rich isotopes of elements 112, 113 and 114 produced in the Act+^{48}Ca reactions—have half-lives from tenths to tens of seconds (figures 6 and 8 below). In the course of consecutive α decays, the partial half-life T_α increases. Half-lives of the isotopes of Rf and Db at the end of decay chains of SHN for which SF was observed reach hours and days. For identification of atomic numbers of SHN the methods of fast chemistry may be applied. In contrast to short-lived products of the cold-fusion reactions, the new region of chemistry of the heaviest elements becomes available.

Most of these methods were applied in experiments on the synthesis of SHN and will be discussed in the following section. Even use of combination of a few methods of identification for the full set of results obtained in the series of experiments aimed at the investigation of SHN allows us to determine unambiguously atomic and mass numbers of synthesized nuclei.

4. Results

4.1. Even-*Z* nuclei

4.1.1. Synthesis and identification of element 114 flerovium. The largest neutron excess in the CN with 114 protons can be achieved in the ^{244}Pu + ^{48}Ca complete-fusion reaction. The first super-heavy nucleus was discovered on June 25, 1999, in experiments performed at the DGFRS by Dubna (FLNR)-Livermore (LLNL) collaboration. Two identical decay chains were observed. Each consisted of two consecutive α decays terminated by SF of the third nucleus (see figure 6). In this experiment, carried out at the lowest projectile energy only, the parent nucleus was assigned to ^{288}Fl [39]. Later on, the cross-section measurement in combination with decay properties of produced nuclei gave correct identification of the mass number of 289 for this isotope of element 114.

In 2003 the study of the ^{244}Pu + ^{48}Ca reaction was continued at higher ^{48}Ca energies [42] (see figure 7). The same isotope was observed at two higher excitation energies. At increased energies, another isotope, ^{288}Fl, with different decay properties was produced also. Its decay chain consisted of α decay

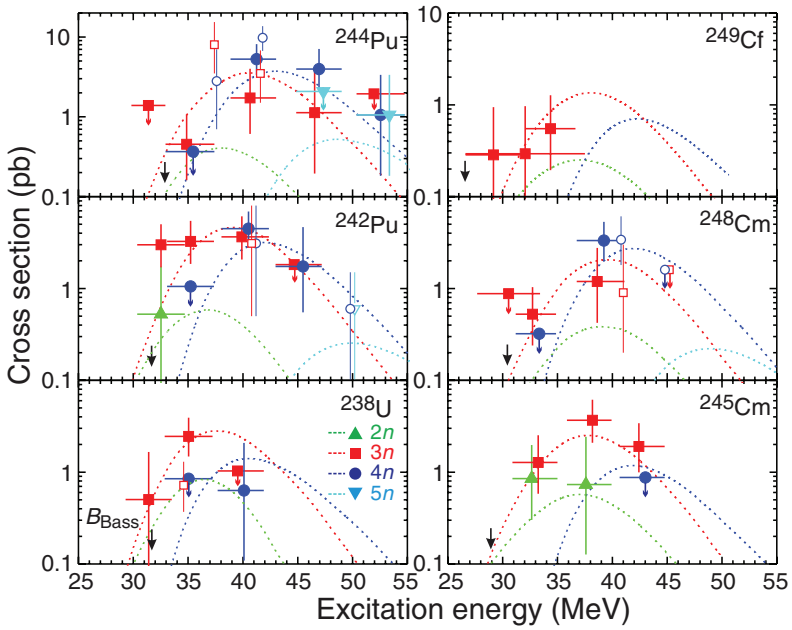

Figure 7. Excitation functions for the 2*n* (green triangle up), 3*n* (red square), 4*n* (blue circle) and 5*n* (cyan triangle down) evaporation channels from the complete-fusion reactions ^{238}U, ^{242,244}Pu, ^{245,248}Cm, ^{249}Cf + ^{48}Ca measured at the DGFRS [39–45] (solid symbols) and the SHIP [50, 51], BGS [52, 53] and TASCA [32, 54] (open symbols). For reference purposes, the Bass barrier [55] is shown by a black arrow in each panel.in the left bottom panel it is labeled with B_{Bass}. Lines show the results of calculations [56–59]. Vertical error bars correspond to statistical uncertainties [60] for the DGFRS experiments and available data for other setups. Horizontal error bars represent the range of excitation energies populated at given beam energy. Position of some symbols were shifted from centers of energy intervals for avoidance of their mixing. Upper cross-section values are shown by colored arrows.

of parent nucleus and SF of daughter nuclide which half-life is lower by factor of 300 than that for daughter isotope in the first decay chain. Finally, at the highest energy the third isotope, ^{287}Fl, was observed. The consideration of decay properties of daughters in the three chains evidently indicated that the second chain should originate from even-*N* nucleus and neighbouring isotopes should have odd number of neutrons. This is explained by the hindrance factor increasing SF half-lives of odd-*N* and odd-*Z* nuclei by a few orders of magnitude that was established for many nuclei (see, e.g. [38]). Such assignment is in agreement with fine structure in α decays of synthesized nuclei, which will be discussed below (see figures 6 and 11).

The measured production cross sections of all the three isotopes agree well with expectations for complete-fusion reactions with evaporation of three, four and five neutrons from CN ^{292}Fl [56–59, 61, 62]. The decay properties of ^{287}Fl were investigated in more detail and the new lighter isotope ^{286}Fl was synthesized in the cross bombardment of ^{242}Pu by ^{48}Ca [44] in 2003. The isotope ^{287}Fl, product of the 5*n*-evaporation channel of the ^{244}Pu + ^{48}Ca reaction, was observed also in the ^{242}Pu(^{48}Ca,3*n*) reaction at the three lowest excitation energies of the CN ^{290}Fl [44] (see figures 6 and 7). Further increase of projectile energy allowed synthesis of the new isotope ^{286}Fl. Its decay chain was similar to that of its heavier even–even neighbour ^{288}Fl, an α decay of ^{288}Fl and SF of daughter nuclide ^{284}Cn. In agreement with theoretical expectations, the stability of nuclei, especially against SF, decreases with receding from the neutron magic number $N = 184$: even–even isotope ^{286}Fl with approximately equal probabilities undergoes α decay and SF.

In the ^{238}U + ^{48}Ca reaction, investigated in 2003–2004 [44], one event of SF was attributed to the decay of ^{282}Cn and seven α-decay chains of ^{283}Cn were detected at three projectile energies (see figures 6 and 7). In one case ^{279}Ds underwent α decay, instead of the more probable SF mode, then two more α decays of ^{275}Hs and ^{271}Sg and SF of ^{267}Rf were registered. A similar long chain was observed in the ^{242}Pu(^{48}Ca, 3*n*)^{287}Fl reaction also [44]. Once again this long decay chain has been registered in the third cross bombardment ^{245}Cm(^{48}Ca, 2*n*)^{291}Lv [42, 45] (see below).

Experiments on the synthesis of Fl isotopes were repeated in other laboratories. A study of the ^{242}Pu + ^{48}Ca fusion reaction at the BGS was published in 2009–2010. One and two decay chains of ^{287}Fl and ^{286}Fl, respectively, were observed [52, 53] with decay modes, half-lives and decay energies in agreement with results published by the DGFRS group [42–45]. Besides, one more decay chain of the lightest isotope ^{285}Fl, product of the 5*n*-evaporation channel of the ^{242}Pu + ^{48}Ca reaction, was found to consist of five consecutive α decays terminated by SF of ^{265}Rf (see figures 6 and 7). In addition, the ^{238}U + ^{48}Ca reaction was studied at one ^{48}Ca energy at the SHIP [50] in 2005–2007. Here two decay chains were measured, which fully confirm data that were previously assigned to the isotope ^{283}Cn in experiments at the DGFRS. Two ER-SF chains were assigned to a 50% SF branch of this isotope; this, however, was not evident from the data where ^{283}Cn was observed as daughter nucleus after α decay of ^{287}Fl [42–45, 52] and the upper limit of 0.1 was set for a SF branch of ^{283}Cn [44]. And finally in 2009, the decay properties of ^{288,289}Fl were also confirmed in experiments [32, 54] performed with use of the TASCA (see figures 6 and 7). In addition, in this work a rare α-decay branch for ^{281}Ds and SF of ^{277}Hs were detected in one decay chain of ^{289}Fl.

In 2011 a joint IUPAC/IUPAP Working Party (JWP) recommended that the Dubna–Livermore collaboration be credited with discovery of the new element 114 produced in the ^{242}Pu(^{48}Ca, 3n)^{287}114 reaction [63]. The element with atomic number 114 was named flerovium (Fl) to honour the Flerov Laboratory of Nuclear Reactions which was founded by Flerov and where super-heavy elements were synthesized [64].

The relatively high stability of ^{283}Cn ($T_{1/2} \approx 4$ s) allowed researchers to investigate for the first time, the chemical properties of element 112. In 2006–2007, the IVO setup was applied for collecting the ^{242}Pu + ^{48}Ca reaction products in the chamber filled by a He/Ar carrier gas which delivered volatile reaction products (including short-lived isotopes of Hg and Rn) to detection system COLD. Here, atoms were deposited according to their interaction with the detector surfaces. The COLD consisted of an array of 32 pairs silicon detectors, with the active surfaces facing each other. The surface of one detector in each of 32 pairs was covered by gold layer. The temperature gradient was established along detectors by a thermostat heating at the inlet and a liquid–nitrogen cryostat cooling near the outlet. The primary fusion-evaporation reaction product ^{287}Fl has a half-life of about 0.5 s which was too short compared with the average transport time from the reaction chamber to the detector. Thus, only the daughter nucleus ^{283}Cn could reach the detector. In these experiments, five decay chains of ^{283}Cn were registered [46, 47]. By directly comparing the adsorption characteristics of ^{283}Cn to that of mercury and the noble gas radon, it was found that the element Cn was more volatile than Hg and unlike radon, reveals a metallic interaction with the gold surface. These adsorption characteristics establish element Cn as a typical element of group 12.

The results of the study of the chemical properties of Fl are less definite. In the first experiment [49] performed in 2007, three decay chains of ^{287,288}Fl were observed in the reactions of ^{48}Ca with ^{242,244}Pu. Their deposition on the detectors with temperature −90, −88 and −4 C indicates that element Fl is at least as volatile as element 112 (noble-gas-like behaviour). In the second work [65] published in 2014, two decay chains were attributed to the ^{244}Pu + ^{48}Ca reaction products ^{288,289}Fl. But both events were observed at room temperature (+21 C) indicating volatile-metalic behaviour of Fl.

4.1.2. Synthesis of element 116 livermorium. The first nucleus of element 116 was discovered at the DGFRS on July 19, 2000 [40, 41]. Like in 1999 experiment ^{244}Pu + ^{48}Ca, the first study of the ^{248}Cm + ^{48}Ca reaction in 2000–2001 was performed at low-energy side of the excitation function [43, 44]. In this series of experiments, three similar decay chains of parent nucleus were observed which were followed by a sequence of two α decays and SF in each case. The decay properties of these descendants were in full agreement with those measured in 1999 in the ^{244}Pu + ^{48}Ca reaction [39]. After measuring the excitation function of the ^{244}Pu + ^{48}Ca reaction [42], ERs observed in the ^{248}Cm + ^{48}Ca reaction were identified as the product of the 3n-evaporation channel, ^{293}Lv.

Investigation of this reaction was continued in 2004 at higher ^{48}Ca energy [43, 44]. Here, like in the case of the ^{244}Pu + ^{48}Ca reaction, increase of the excitation energy allowed us to observe simultaneously two isotopes: ^{293}Lv and a new lighter isotope ^{292}Lv. If the same type of nuclear reaction occurred in both cases, then after α decay of the parent nuclei in the reaction with ^{248}Cm the descendant isotopes should be the same as those observed in primary reaction with ^{244}Pu. Indeed, decay properties of the daughter nuclei in the ^{248}Cm + ^{48}Ca reaction were identical to those registered directly in the reaction with ^{244}Pu [39, 42] (see figures 6 and 7).

Experiments were continued with a ^{245}Cm target. In 2003, at the first (lowest) bombarding energy two new isotopes of element 116 were synthesized [42]. The decay properties of daughter nuclei in one of these were in agreement with those observed in the ^{244}Pu(^{48}Ca, 5n)^{287}Fl and ^{242}Pu(^{48}Ca, 3n)^{287}Fl [42–44] as well as in the ^{238}U(^{48}Ca, 3n)^{283}Cn [44] reactions. The α decay of the second isotope lead to decay chains seen in the ^{242}Pu(^{48}Ca, 4n)^{286}Fl [44] and ^{238}U(^{48}Ca,4n)^{282}Cn [44] reactions. This indicates observation of the 2n- and 3n-evaporation channels of the ^{245}Cm + ^{48}Ca reaction, i.e. ^{291}Lv and ^{290}Lv, respectively (see figures 6 and 7). In 2005, further increase of ^{48}Ca energy resulted in a reduction in the yield of ^{291}Lv and increase of that of ^{290}Lv [45]. Finally, at the highest energy, only 3n-evaporation channel was observed. Such variation of production cross sections of two isotopes is in agreement with what it should be expected for the behaviour of the xn channels of the complete-fusion reactions. The decrease of the neutron number in the target nuclei, e.g. from ^{244}Pu to ^{242}Pu or from ^{248}Cm to ^{245}Cm, results in rise of the neutron binding energy and somewhat lower excitation energy of CN at the fusion barrier (figure 7). This leads to a relative increase in the yields of lower xn channels. Note, the 2n-evaporation channel was also observed in two other reactions with somewhat lower-N target nuclei. A single decay chain was assigned to the 2n-reaction product in the experiment with ^{242}Pu [44] (figure 7) and four chains were observed in the ^{243}Am(^{48}Ca, 2n)^{289}115 reaction [66] (see below).

Owing to strong correlations in three α-decay chains of ^{291}Lv with following ^{287}Fl and lighter descendants (even up to ^{267}Rf in one chain), the IUPAC/IUPAP JWP recommended that the Dubna–Livermore collaboration be credited with discovery of element 116 [63]. The element with atomic number 116 was named livermorium (Lv) in honour of the Lawrence Livermore National Laboratory because of experiments on the synthesis of super-heavy elements, including element 116, were performed in collaboration with group of researchers from this laboratory [64].

The independent confirmation of the results obtained at the DGFRS in 2000, 2001 and 2004 in the ^{248}Cm + ^{48}Ca reaction [40, 41, 43, 44], where element 116 was observed for the first time, followed in 2007 in the SHIP experiments [51]. Four and one decay chains of ^{292}Lv and ^{293}Lv, respectively, were registered at the excitation energy of 40.9 MeV (see figures 6 and 7). The decay properties of the parent and all the descendant nuclei are in agreement with those measured at the DGFRS. One more chain was not definitely assigned. The energy and lifetime of the first α decay agree with data determined for ^{293}Lv but energies of the next three α particles are larger than those measured for ^{289}Fl, ^{285}Cn [39–42] and ^{281}Ds [32, 54] as well as much longer decay time was observed for the terminating

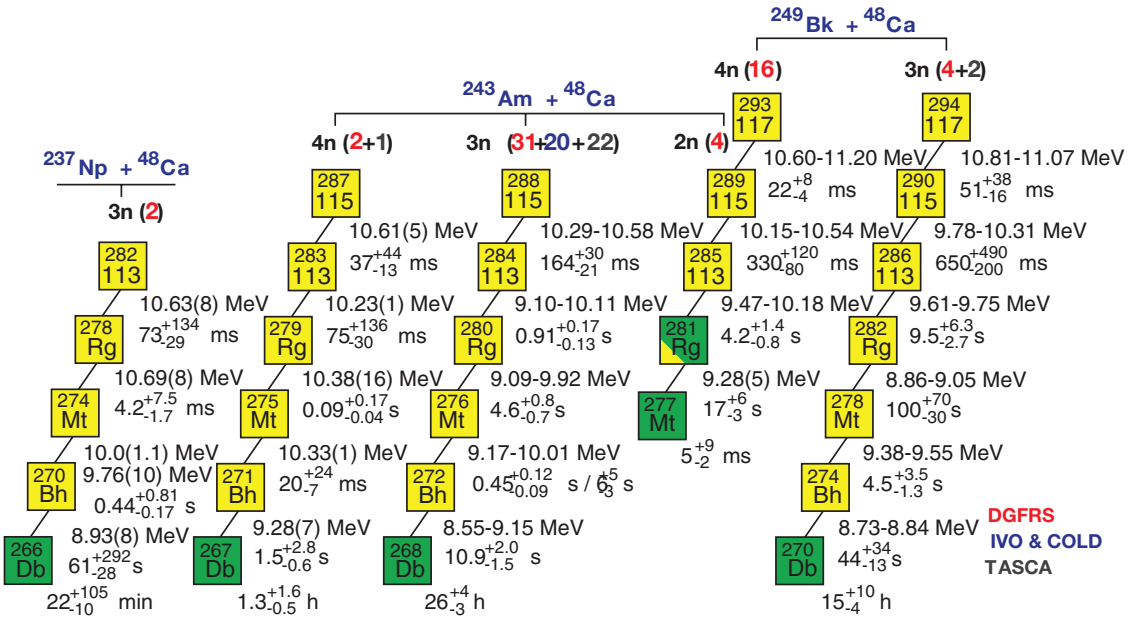

Figure 8. Summary decay properties of the isotopes of odd-*Z* elements observed among the products of ^{48}Ca beam and ^{237}Np, ^{243}Am and ^{249}Bk target reactions. The numbers of the decay chains of the given isotopes, the products of corresponding *xn*-evaporation channels, observed in experiments with use of the DGFRS [26, 27, 34, 36, 66–70] (in red), chemical setup (in blue) [26, 71, 72] and TASCA (in grey) [73, 74] are shown. The average energies or energy intervals of α particles and half-lives are given for all α emitters observed in these experiments (yellow squares). The energy uncertainties given in brackets correspond to the data with the best energy resolution. For spontaneously fissioning nuclei marked by green squares the half-lives are listed.

fission event than that seen at the TASCA experiment [32, 54]. The decay properties of detected nuclei are in good agreement with those observed in long decay chains originating from ^{291}Lv which could be produced in the 5*n*-evaporation channel of the reaction with ^{248}Cm or in the reaction with lighter Cm isotope, e.g. ^{246}Cm (percentage of 3.1%) (private communication by Hofmann). Indeed, α-particle energies and lifetimes of the second to fourth detected nuclei coincide well with data for ^{287}Fl, ^{279}Ds and ^{275}Hs as well as decay time of SF nucleus is in agreement with half-life for ^{271}Sg (see figure 6). Somewhat lower α-particle energy for the parent even-odd ^{291}Lv and missing of one of five decays (^{283}Cn) are quite possible.

4.1.3. Synthesis of element 118. For the first time, the decay chain of the element 118 was synthesized on March 19, 2002, in the reaction ^{249}Cf(^{48}Ca, 3*n*)^{294}118 studied at the DGFRS [45]. Two more decay chains of ^{294}118 were observed in 2005 at higher projectile energy [45]. Finally, the fourth decay chain of the same isotope was registered during two experiments aimed at the synthesis of element 117 in the ^{249}Bk + ^{48}Ca reaction performed in 2009–2010 and 2012 [36] [2]. Identification of the isotope ^{294}118 was based on the results of the four cross reactions: ^{249}Cf(^{48}Ca, 3*n*)^{294}118 → ... → ^{282}Cn [45], ^{245}Cm(^{48}Ca, 3*n*)^{290}Lv → ... → ^{282}Cn [42, 45], ^{242}Pu(^{48}Ca, 4*n*)^{286}Fl → ^{282}Cn [44] and ^{238}U(^{48}Ca, 4*n*)^{282}Cn [44] (see figure 6). Among the daughter nuclei in the decay chain of ^{294}118, decay properties of two isotopes ^{286}Fl and ^{282}Cn were confirmed in independent experiments at the BGS [52, 53] (see subsection 4.1.1. above).

[2] In the course of the long-term work, ^{249}Cf—the product of β^- decay of ^{249}Bk (330 d)— is being accumulated in the target. The gradual ingrowth of ^{249}Cf in the ^{249}Bk target material during both series of experiments resulted in production of ^{294}118 with cross section comparable with values measured for the ^{249}Cf(^{48}Ca, 3*n*) reaction at close excitation energies (see figures 6 and 7).

4.2. Odd-Z nuclei

4.2.1. Synthesis and identification of elements 113 and 115. The discoveries of elements 113 and 115 as the products of the complete-fusion reaction ^{243}Am + ^{48}Ca that led to the synthesis of isotopes of element 115 and their α-decay product, element 113 that was also unknown at that time, were reported in 2004 [67]. The first decay chain was observed at the DGFRS on 24 July, 2003. This involved two new elements at once, ^{288}115 and ^{284}113, followed by α decays of three new neutron-rich isotopes of the known elements ^{280}Rg, ^{276}Mt and ^{272}Bh and SF of ^{268}Db (see figure 8). The electron-capture (EC) of ^{268}Db leading to presumably rapid SF of ^{268}Rf (T_{SF} ~ 1 s [7]) could not be excluded as well. The run was performed at two projectile energies, which resulted in observation of two isotopes ^{288}115 and ^{287}115 as well as their descendant nuclides down to ^{268}Db and ^{267}Db (figure 8). In the ^{243}Am + ^{48}Ca reaction, the energies of the bombarding particles and reaction cross sections were comparable with results of experiments where excitation functions for the reactions ^{242,244}Pu, ^{245,248}Cm + ^{48}Ca have been measured (see figures 7 and 9). Two neighbouring isotopes of the new element were detected at different ^{48}Ca energies, in agreement with expectations for the fusion-evaporation reactions. After observing decays of the three nuclei ^{288}115 at the excitation energy $E^* \approx 40$ MeV, with the increase of energy to $E^* \approx 45$ MeV a new decay chain originating from different isotope was registered [26, 67] (see, e.g. the difference in

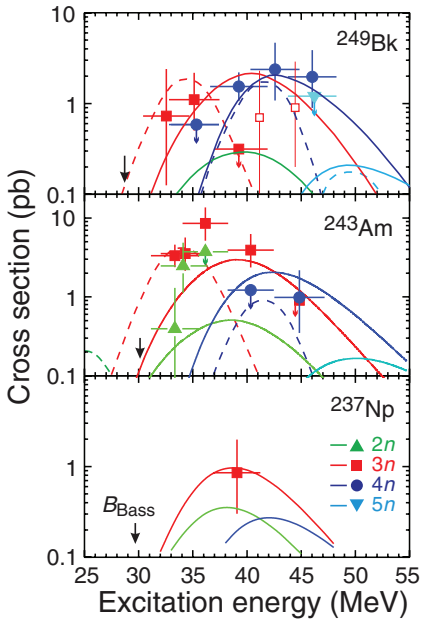

Figure 9. Excitation functions for the 2*n* (green triangle up), 3*n* (red square), 4*n* (blue circle) and 5*n* (cyan triangle down) evaporation channels from the complete-fusion reactions ^{237}Np, ^{243}Am, ^{249}Bk + ^{48}Ca measured at the DGFRS [26, 27, 34, 36, 66–70] (solid symbols) and TASCA [74] (open symbols). For reference purposes, the Bass barrier [55] is shown by black arrow in each panel; in the bottom panel it is labeled with B_{Bass}. Vertical error bars correspond to statistical uncertainties [60] for the DGFRS experiments and available data from TASCA. Horizontal error bars represent the range of excitation energies populated at given beam energy. Symbols with arrows show upper cross-section limits. The results of theoretical calculations are shown by solid [56–59] and dashed [61] lines.

half-lives of the neighbouring ^{280,}Rg and ^{279}Rg, ^{276}Mt – ^{275}Mt and other descendant nuclei in figure 8). The decay properties of SHN will be discussed in the following section but here we emphasize that the decay properties of nuclei observed in the ^{243}Am + ^{48}Ca reaction evidently differ from those produced in the reactions with even-*Z* target nuclei. One can compare figures 6 and 8 where isotopes of odd-*Z* elements show decay properties intermediate between those of neighboring even-*Z* nuclei.Their decay chains are longer which is caused by unpaired protons increasing stability of nuclei against SF by orders of magnitude, etc.

In addition to the above-mentioned measurements, a chemical experiment was performed for identification of the long-living SF isotope ^{268}Db that was observed after five sequential α decays of ^{288}115 nuclei [71]. The ^{243}Am target was bombarded by ^{48}Ca ions with an energy corresponding to 247 MeV in the middle of the target that means E^* = 39 MeV for the CN ^{291}115 (compare with the DGFRS data in figure 9). On leaving the target, the recoiling nuclei passed through a collimator suppressing the yield of transfer-reaction products (capture angle of ±12.5°) and were stopped in a copper catcher. Each one–two days the front layer of catcher with a thickness exceeding range of ERs was mechanically cut from the surface. This part of the catcher could contain ^{268}Db (T_{SF} ~ 1 d) atoms. Then elements of group 4 and 5 were isolated from actinides [71].

The test experiments [75] have shown that the factor of separation of transactinides from actinides was more than 10^4. On the other hand, from two possible transactinides with Z = 104 and 105, the element of group 4 (Rf) preceded by five α decays could be produced in the ^{243}Am + ^{48}Ca reaction only in the *pxn* channel or as a result of EC/ β^+ decay of one of elements 115-Bh. However, the *pxn* channel for x = 1–5 or EC/ β^+ decay of ^{288}115 or ^{284}113 would lead to the now known isotopes of Fl or Cn whose decay chains strongly differ from the observed ones (see figures 6 and 8). The EC/β^+ decay of lighter descendants ^{280}Rg–^{272}Bh leads to even–even isotopes ^{280}Ds–^{272}Sg for which SF is expected with half-lives less than 1 s (see [7] and figure 13 below). Therefore, the ~1-d SF, if observed in transactinides fraction, could originate from the element of group 5 (Db) only (direct SF or SF with short half-life following EC). In 2004, in the chemical experiment [71] 15 SF events of the nuclei of a transactinide element were detected. These showed a half-life of 32^{+11}_{-7} h, high total kinetic energy of SF fragments (~235 MeV) and average neutron multiplicity per fission act (4.2) and were produced with a cross section of about 4.2 pb. All the values, within experimental errors, are in agreement with those ($T_{1/2}$, TKE, σ_{3n}) measured for ^{268}Db at the DGFRS in 2003 [67] and later experiments [66, 70] (figures 8 and 9). These results were later (in 2005 [72]) corroborated in another chemical experiment that attempted studying more delicate chemical properties of Db within group 5.

In chemistry experiments [71, 72] the SF activity was produced in the *same* ^{243}Am + ^{48}Ca reaction (I) at the *same* projectile energy (II) with the *same* decay properties (namely, decay mode (III), half-life (IV), total kinetic energy (V)) and the *same* cross section (VI) as it was observed in the experiment performed at the DGFRS [67]. All the factors allowed one to conclude that one and the same isotope has been observed in both the physical and chemical experiments [26, 67, 71, 72]. Simultaneously, all the precursors (Z = 107, 109, 111, 113 and 115) discovered in [67] were identified by the method of genetic relation between ancestor and descendant [37]. In our further investigation of the region of odd-*Z* SHN we studied neutron-deficient isotopes and continued, as well, the ^{243}Am + ^{48}Ca experiment in a more extended range of projectile energies for observation of more nuclei and detailed measurement of the excitation function of this reaction. In 2006 in the ^{237}Np(^{48}Ca, 3*n*) reaction, we observed two decay chains originating from the lighter odd–odd isotope ^{282}113 [68] (figure 8). Decay properties of ^{282}113 and its descendant nuclei ^{278}Rg, ^{274}Mt, ^{270}Bh and ^{266}Db were in full agreement with those following from decay properties of heavier isotopes ^{283,284}113 and other descendants previously produced in the ^{243}Am + ^{48}Ca reaction.

In contrast to even-*Z* target nuclei, application of the cross-bombardment method for odd-*Z* nuclei is limited by the number of target nuclei available for experiments, that is ^{237}Np, ^{241,243}Am and ^{249}Bk. The ^{249}Bk(^{48}Ca, 3-4*n*) reactions lead to heavier isotopes of element 115 and their descendants; therefore only the isotope ^{289}115, the product of the 2*n*-evaporation channel of the reaction ^{243}Am + ^{48}Ca, seems to be useful for cross-bombardment experiments. In 2010–2012, with aim of synthesizing this isotope as well as measuring excitation

function in a wider energy range, we performed a new series of experiments with ^{243}Am [66, 70]. The results of all these experiments are presented in figures 8 and 9. Indeed, at the two lowest ^{48}Ca energies, we detected the product of the 2*n*-reaction channel, ^{289}115, undergoing two consecutive α decays and terminated mainly by SF of ^{281}Rg, as it was observed for the same nuclei synthesized in the reaction ^{249}Bk + ^{48}Ca (see below). These chains were not detected at higher ^{48}Ca energies.

In sum with results of 2003, at four energies, 31 decay chains of ^{288}115, product of the evaporation of three neutrons, with maximum yield at the excitation energy of about 36 MeV, were registered. At the energy $E^* \approx 45$ MeV, we detected two decay chains of ^{287}115 that were not found at lower ^{48}Ca energies. Such a behaviour of $\sigma_{xn}(E^*)$ is expected for cooling process of exited CN ^{291}115 and is in full agreement with numerous similar observations for fusion-evaporation reactions[3]. The radioactive decay properties of ^{288}115, ^{287}115 and their daughter nuclei discovered in 2003 [26, 67] were completely confirmed by registration of 28 new decay chains in the new series of experiments [66, 70].

In four decay chains of ^{288}115, α decay of ^{268}Db was searched for within beam-off intervals from 2.7 h up to 1–3 d following decay of ^{272}Bh (see discussion in [34]). No events were found with E_α = 7.7–8.2 MeV which could be expected for ^{268}Db. This result is in agreement with chemistry experiments [71, 72] where SF activity was found in the fraction of transactinide elements. Thus, an upper limit of 7% can be set for α-decay branch b_α for ^{268}Db.

In 2012, the same ^{243}Am + ^{48}Ca reaction was studied at two close beam energies of 242.1 and 245.0 MeV (E^* = 35.1 and 37.5 MeV) at the TASCA [73] applying a high-resolution α, x-ray and γ-ray coincidence spectroscopy technique. In total, thirty correlated α-decay chains were detected which contain five ER-α-α-SF and two ER-α-SF events 'compatible with decay chains proposed to originate from either ^{289}115 or ^{288}115 [73]'. The excitation function of the reaction was not measured in this experiment; short decay chains and reasons for doubts about their assignment are not given in [73]. One long chain of five α decays was clearly compatible with the characteristics of the decay chain attributed to start from the isotope ^{287}115 [66, 67]. The remaining 22 chains are compatible with the 31 chains previously assigned to the decay of ^{288}115 [26, 66, 67, 70]. Here α decay of ^{268}Db was not observed as well. An upper limit $b_\alpha \leq 4\%$ follows from results of all these experiments. The cross-section values are not given in [73]. The summary decay properties of ^{287,288}115 are shown in figure 8.

In both experiments at the DGFRS [26, 66, 67, 70] and TASCA [73], complex spectra of the α-particle energy were measured (see figure 12 below). In decay of ^{276}Mt, that shows the most complex α-particle spectrum, we could not exclude observation of two states with different lifetimes [66]. Despite the single half-life for ^{276}Mt proposed in [73], its decay time in one chain was t = 8.95 s whereas the average lifetime for other 15 events was τ = 0.55 s (probability to decay with $t \geq 8.95$ s for 16 events with τ = 0.55 s is only 1.5×10^{-6}). Thus, this new long decay time just could confirm the assumption of [66]. In figure 8 we present result of a two-exponential fit [76] of all the available data for ^{276}Mt which suggests two half-lives. However, more statistics is still needed for definite conclusion.

In addition to studying the formation and radioactive properties of the products of the ^{243}Am + ^{48}Ca reaction, the TASCA experiment [73] was aimed at the measuring x- and γ-rays in coincidence with α particles of nuclei starting from element 115. In one decay chain the escape event with E = 0.825 MeV was 'firmly attributed' to ^{276}Mt (probability of its random origin is not given in [73]) and was coincident with two Ge-detector entries at 136 and 167 keV, which are consistent with Z = 107 $K_{\alpha 2}$ and K_β energies, respectively [77]. Because of 10–15% probability of random α-photon coincidences, authors noted that either one or both of events can also represent γ-rays or Compton scattered or background events. Besides, several α–γ coincidences were observed for ^{280}Rg and ^{276}Mt.

In spite of the fact that registration of x-rays in coincidence with α particles of ^{276}Mt was not definitely established, the experiment demonstrated the prospects for investigation of nuclear structure of SHN. However, these studies call for considerable increase of production rate of nuclei which could be reached at the new experimental facilities which are planned to be put into operation in a few years (see section 5).

4.2.2. Synthesis of element 117. The synthesis of heavier element 117 became feasible when 22.2 mg of the ^{249}Bk target material was produced at the High Flux Isotope Reactor (HFIR) at the Oak Ridge National Laboratory (ORNL) [27] and sent to Dubna. For the first time, element 117 was observed at the DGFRS on August 20, 2009, in the complete-fusion reaction ^{249}Bk(^{48}Ca, 4*n*)^{293}117 [69].

In 2009–2010, at two projectile energies corresponding to the excitation energies of the CN ^{297}117 of 39 and 35 MeV, we synthesized two isotopes of element 117 [27, 69] (see figures 8 and 9). At the excitation energy of 39 MeV that corresponds to the expected maximum for production yield of the 4*n*-evaporation channel we have registered five decay chains of the odd-even isotope ^{293}117. From the well established behavior of the excitation functions measured for numerous reactions, it followed that a reduction of the projectile energy should result in a decrease of the cross section for the 4*n* channel and increase of the cross section of a heavier odd–odd isotope with lower α-particle energy and longer lifetime. Indeed, at 35 MeV excitation energy, we produced one longer decay chain of the isotope ^{294}117. As was expected for an odd–odd nucleus, fission of ^{282}Rg and ^{278}Mt is suppressed because of the unpaired neutrons compared to α emission and gives a longer α chain.

Identification of isotopes of the new element 117 was made similarly to that of the isotopes with Z = 115 produced in the ^{243}Am(^{48}Ca, 2-4*n*)$^{287\text{-}289}$115 reaction. Neutron-rich ^{290}115 and ^{289}115 that are daughters of α decay of the isotopes of element 117, produced in the ^{249}Bk(^{48}Ca,3-4n)^{294,293}117 reaction should have lower α-particle energies and respectively, longer lifetimes

[3] The products of the 2*n*-evaporation channel of the ^{242}Pu, ^{245}Cm + ^{48}Ca reactions, isotopes ^{288}Fl and ^{291}Lv, were observed in our experiments with comparable cross sections at E^* = 32–38 MeV [42–45] (figure 7).

compared with the isotopes $^{288}115$ and $^{287}115$ produced in the reaction with ^{243}Am. Indeed, α-decay energies of all the descendant nuclei $^{289,290}115$, $^{285,286}113$, ^{282}Rg, ^{278}Mt and ^{274}Bh (products of the ^{249}Bk + ^{48}Ca reaction) have smaller E_α and longer T_α when compared with neighboring isotopes $^{287,288}115$, $^{282-284}113$, $^{278-280}$Rg, $^{274-276}$Mt and $^{270-272}$Bh observed in the reactions with ^{243}Am and ^{237}Np (see figures 8 and 12 below). Moreover, analogously to lighter isotopes of odd-Z nuclei with $Z \leq 111$ and $N \leq 163$, the α-decay energies of all the products of the reaction with ^{249}Bk including parents $^{293}117$ and $^{294}117$ have intermediate values between those measured for neighboring even-Z nuclei (see figures 6, 8, 11 and 12 below).

The number of consecutive α decays originating from $^{289}115$ and $^{288}115$ differ. Decay chains of $^{289}115$ are terminated mainly by SF of ^{281}Rg but all 31 [26, 66, 67, 70] and 22 [73] observed decay chains of $^{288}115$ ends in SF of ^{268}Db (figure 8). Furthermore, in spite of complex α-particle spectra of odd-Z nuclei, decay properties of $^{289}115$ and $^{288}115$ and descendant nuclei are different (compare T_α values for nuclei in figure 8 and shape of α-particle spectra in figure 12 below, especially for isotopes of element 113). At the same time, α-particle energies, decay times and decay modes of isotopes $^{289}115$, $^{285}113$, and ^{281}Rg observed in the reactions with ^{243}Am and ^{249}Bk agree. Therefore, one can conclude that isotope $^{289}115$ was produced in cross reactions with two target nuclei to provide cross bombardment evidence for the discovery of the new elements 113,115 and 117.

These conclusions were confirmed also by the following experiments aimed at the measurement of excitation functions for isotopes of element 117 [34, 36]. In 2012 the ^{249}Bk + ^{48}Ca reaction was studied at five excitation energies within interval E^* = 30.4–48.3 MeV. In two campaigns with ^{249}Bk target four decay chains of $^{294}117$ were produced at two laboratory-frame beam energies E_{lab} = 244 and 247 MeV (E^* = 32.6 and 35.1 MeV) and 16 chains of $^{293}117$ were observed at three higher energies E_{lab} = 252, 256 and 260 MeV (E^* = 39.3, 42.6 and 46.0 MeV) (see figures 8 and 9) providing additional evidence of the identification of the nuclei of element 117.

The same reaction was studied in 2012 at the TASCA at ^{48}Ca energies of 252, 254 and 258 MeV [74]. In total, four decay chains, two long and two shorter ones (not published yet), all terminated by SF, were observed. The decay properties of the nuclei in the long chains registered at the two largest ^{48}Ca energies and assigned to $^{294}117$ are in good agreement with results reported from the DGFRS group. In addition, in both chains events with E_α = 7.89 and 7.90 MeV were found 1.3 h and 1.6 h after α decay of ^{274}Bh and assigned to ^{270}Db (T_α = 1 h) followed by SF of ^{266}Lr (T_{SF} = 11 h). This was not observed in experiments at the DGFRS and needs a short comment.

Consecutive α decays of nuclei $^{288}115$–^{272}Bh or $^{294}117$–^{274}Bh in all the observed decay chains occurred within 2 and 7 min, respectively. The probability of random observation of any of daughter nuclei with E_α = 8.5–10.5 MeV (see figures 5 and 12 below) within beam-off interval of 10 min at the DGFRS was about 2.5 × 10^{-3} (at E_{lab} = 243 MeV in [66, 70]) and 2.8 × 10^{-4} (at E_{lab} = 247 MeV in [34, 36]). But the situation differs at the end of decay chains where the time interval between the last α particle and SF increases up to hours and tens of hours. The probability of the appearance of a random α particle within this interval increases accordingly.

However, the probability of the random origin P_{err} of events within some energy range (e.g. E_α = 7.7–8.2 MeV in [34]) and relatively long time interval, say 2 h, was not presented in [74]. The given total numbers of beam-off α particles with E_α = 6–12 MeV in the detector pixels where decay chains were observed [74] results in a rather large P_{err} value of 0.5. Furthermore, one could expect similar decay properties for ^{270}Db (N = 165) and ^{268}Db (N = 163) which follows from close predicted Q_α values (8.31 and 8.26 MeV, respectively [78]) as well as from comparable α-decay half-lives of other N = 163, 165 isotopes ^{269,271}Sg and ^{270,272}Bh (see figures 6 and 8 and table 1 below). But, as mentioned above, α decay of ^{268}Db was not seen in the DGFRS [26, 66, 67, 70], TASCA [73] and chemistry experiments [71, 72]. Thus, the partial T_α value for ^{268}Db exceeding that for ^{270}Db, suggested in [74], by more than two orders of magnitude (≥300 h) seems to be very unlikely. That is why we do not include results for ^{270}Db in figure 8 and below until finishing detailed analysis of the data ([36] in [74]).

4.3. Attempts to produce Z = 119 and 120 nuclei

By now, ten reactions of actinide target nuclei ^{233,238}U, ^{237}Np, ^{242,244}Pu, ^{243}Am, ^{245,248}Cm, ^{249}Bk and ^{249}Cf with ^{48}Ca were used for investigation of the region of SHN. In the ^{233}U + ^{48}Ca reaction no decay chains were observed with an upper cross section limit of 0.6 pb [44]. Nine other reactions resulted in synthesis of 25 even-Z and 29 odd-Z nuclei.

The decay properties of these nuclei revealed a significant increase in their stability as they approached the predicted neutron shell N = 184. The nuclides with the largest neutron and proton numbers that were synthesized in reactions with the heaviest target nuclei ^{248}Cm, ^{249}Bk and ^{249}Cf that are ^{293}Lv (N = 177), $^{294}117$ (N = 177) and $^{294}118$ (N = 176), respectively, still possess 7–8 fewer neutrons than the predicted magic number N = 184. One can expect that increasing the number of neutrons in these nuclei would result in further increase of their stability. Unfortunately, nuclides with $Z > 98$ do not exist in quantities sufficient for producing targets for these types of experiments. Therefore, isotopes with larger neutron excess can be reached only if they are formed as heavier ERs. For this purpose, one needs to use complete-fusion reactions with projectiles heavier than ^{48}Ca. One should also note that increasing the atomic number brings us closer to the closed proton shell at Z = 120–126 predicted by some microscopic models, which could also increase shell effects. However, most calculations predict much lower cross sections for complete-fusion reactions with projectiles heavier than ^{48}Ca [59, 61, 62, 79–83].

In 2007 the ^{244}Pu(^{58}Fe, xn)$^{302-x}120$ reaction was studied at the DGFRS [84]. No decay chains consistent with fusion-evaporation reaction products were observed during an irradiation with a beam dose of 0.7 × 10^{19} 330 MeV ^{58}Fe projectiles. The sensitivity of the experiment corresponds to a cross section of 0.4 pb for the detecting a single decay; the upper cross-section limit was set at 1.1 pb. In 2007–2008 a more symmetric reaction ^{238}U + ^{64}Ni leading to the same CN was used at the SHIP [85].

Table 1. Decay properties of nuclei.

Z	N	A	No. observed [a]	Decay mode, branch [b]	Half-life [c]	E_α (MeV)	Q_α^{exp} (MeV)	Q_α^{th} (MeV)
118	176	294	4 (4/4)	α	$0.69^{+0.64}_{-0.22}$ms	11.66 ± 0.06	11.82 ± 0.06	12.11
117	177	294	5 (5/5)	α	51^{+38}_{-16}ms	10.81–11.07	11.18 ± 0.04	11.43
	176	293	15 (15/15)	α	22^{+8}_{-4}ms	10.60–11.20	11.32 ± 0.05	11.53
116	177	293	5 (5/5)	α	57^{+43}_{-17}ms	10.56 ± 0.02	10.71 ± 0.02	11.09
	176	292	9 (8/7)	α	13^{+7}_{-4}ms	10.63 ± 0.02	10.78 ± 0.02	11.06
	175	291	4 (4/4)	α	19^{+17}_{-6}ms	10.74 ± 0.07 10.50 ± 0.02	10.89 ± 0.07	10.91
	174	290	11 (11/11)	α	$8.3^{+3.5}_{-1.9}$ms	10.85 ± 0.07	11.00 ± 0.07	11.08
115	175	290	6 (5/6)	α	650^{+490}_{-200}ms	9.78–10.31	10.41 ± 0.04	10.65
	174	289	16 (15/16)	α	330^{+120}_{-80}ms	10.15–10.54	10.49 ± 0.05	10.74
	173	288	46 (41/46)	α	164^{+30}_{-21}ms	10.29–10.58	10.63 ± 0.01	10.95
	172	287	3 (3/3)	α	37^{+44}_{-13}ms	10.61 ± 0.05	10.76 ± 0.05	11.21
114	175	289	16 (14/16)	α	$1.9^{+0.7}_{-0.4}$s	9.84 ± 0.02 9.48 ± 0.08	9.98 ± 0.02	10.04
	174	288	35 (31/30)	α	$0.66^{+0.14}_{-0.10}$s	9.93 ± 0.03	10.07 ± 0.03	10.32
	173	287	19 (18/17)	α	$0.48^{+0.14}_{-0.09}$s	10.03 ± 0.02	10.17 ± 0.02	10.56
	172	286	27 (22/14)	α:0.6 SF:0.4	$0.12^{+0.04}_{-0.02}$s	10.21 ± 0.04	10.35 ± 0.04	10.86
	171	285	1 (1/0)	α	$0.13^{+0.60}_{-0.06}$s			11.11
113	173	286	6 (5/6)	α	$9.5^{+6.3}_{-2.7}$s	9.61–9.75	9.79 ± 0.05	9.98
	172	285	17 (17/17)	α	$4.2^{+1.4}_{-0.8}$s	9.47–10.18	10.01 ± 0.04	10.21
	171	284	47 (39/47)	α	$0.91^{+0.17}_{-0.13}$s	9.10–10.11	10.12 ± 0.01	10.68
	170	283	2 (2/2)	α	75^{+136}_{-30}ms	10.23 ± 0.01	10.38 ± 0.01	11.12
	169	282	2(2/2)	α	73^{+134}_{-29}ms	10.63 ± 0.08	10.78 ± 0.08	11.47
112	173	285	17 (16/16)	α	28^{+9}_{-6}s	9.19 ± 0.02	9.32 ± 0.02	9.49
	172	284	37 (34/-)	SF	98^{+20}_{-14}ms			9.76
	171	283	33 (23/31)	α:1. SF: ≤ 0.1	$4.2^{+1.1}_{-0.7}$s	9.53 ± 0.02 9.33 ± 0.06 8.94 ± 0.07	9.66 ± 0.02	10.16
	170	282	14 (14/-)	SF	$0.91^{+0.33}_{-0.19}$ms			10.68
	169	281	1 (1/1)	α	$0.10^{+0.46}_{-0.05}$s	10.31 ± 0.04	10.46 ± 0.04	11.21
111	171	282	6 (6/6)	α	100^{+70}_{-30}s	8.86–9.05	9.16 ± 0.03	9.85
	170	281	20 (17/2)	α:0.1 SF:0.9	17^{+6}_{-3}s	9.28 ± 0.05	9.41 ± 0.05	10.48
	169	280	45 (41/42)	α	$4.6^{+0.8}_{-0.7}$s	9.09–9.92	9.91 ± 0.01	10.77
	168	279	3 (2/2)	α	90^{+170}_{-40}ms	10.38 ± 0.16	10.53 ± 0.16	11.08
	167	278	2 (2/2)	α	$4.2^{+7.5}_{-1.7}$ms	10.69 ± 0.08	10.85 ± 0.08	11.30
110	171	281	17 (17/1)	α:0.07 SF:0.93	$12.7^{+4.0}_{-2.5}$s	8.73 ± 0.03	8.85 ± 0.03	9.30
	169	279	36 (31/4)	α:0.1 SF:0.9	$0.21^{+0.04}_{-0.04}$s	9.71 ± 0.02	9.85 ± 0.02	10.24
	167	277	1 (1/1)	α	$0.006^{+0.027}_{-0.003}$s	10.57 ± 0.04	10.72 ± 0.04	10.79
109	169	278	5 (5/5)	α	$4.5^{+3.5}_{-1.3}$s	9.38–9.55	9.58 ± 0.03	9.55
	168	277	2 (2/-)	SF	5^{+9}_{-2}ms			9.84
	167	276	43 (43/41)	α	$0.45^{+0.12}_{-0.09}$s 6^{+5}_{-3}s	9.17–10.01	10.03 ± 0.01	10.09
	166	275	3 (3/3)	α	20^{+24}_{-7}ms	10.33 ± 0.01	10.48 ± 0.01	10.34
	165	274	2 (2/2)	α	440^{+810}_{-170}ms	10.0 ± 1.1 9.76 ± 0.10	10.2 ± 1.1	10.63
108	169	277	1 (1/1)	SF	3^{+15}_{-1}ms			9.03
	167	275	4 (4/4)	α	$0.20^{+0.18}_{-0.06}$s	9.31 ± 0.02	9.45 ± 0.02	9.41
	165	273	1 (1/1)	α	$0.2^{+1.2}_{-0.1}$s	9.59 ± 0.04	9.73 ± 0.04	9.78

(*Continued*)

Table 1. (*Continued*)

Z	N	A	No. observed [a]	Decay mode, branch [b]	Half-life [c]	E_α (MeV)	Q_α^{exp} (MeV)	Q_α^{th} (MeV)
107	167	274	6 (5/6)	α	44^{+34}_{-13}s	8.73–8.84	8.94 ± 0.03	8.83
	165	272	44 (39/44)	α	$10.9^{+2.0}_{-1.5}$s	8.55–9.15	9.18 ± 0.01	9.08
	164	271	2 (2/2)	α	$1.5^{+2.8}_{-0.6}$s	9.28 ± 0.07	9.42 ± 0.07	9.07
	163	270	1 (1/1)	α	61^{+292}_{-28}s	8.93 ± 0.08	9.06 ± 0.08	8.63
106	165	271	4 (4/2)	α:0.6 SF:0.4	$1.6^{+1.5}_{-0.5}$min	8.54 ± 0.08	8.67 ± 0.08	8.71
	163	269	1 (1/1)	α	2^{+10}_{-1}min	8.57 ± 0.10	8.70 ± 0.10	8.32
105	165	270	6 (6/-)	SF [e]	15^{+10}_{-4}h			8.11
	163	268	66 (66/-)	SF [e]	26^{+4}_{-3}h [d]			7.80
	162	267	3 (3/-)	SF [e]	$1.3^{+1.6}_{-0.5}$h			7.41
	161	266	1 (1/-)	SF [e]	22^{+105}_{-10}min			7.52
104	163	267	2 (2/-)	SF	$1.3^{+2.3}_{-0.5}$h			
	161	265	1 (1/-)	SF	2^{+8}_{-1}min			7.27

[a] Number of observed decays and number of events used for calculations of half-lives / α-particle energies, respectively.
[b] Branching ratio is not shown if only one decay mode was observed.
[c] Error bars correspond to 68%-confidence level.
[d] The value obtained combining the results of physical and chemical experiments.
[e] The SF mode was observed but EC/β^+ or α decay is not excluded.

No events originating from isotopes of element 120 were observed. Measured upper cross-section limit of 0.09 pb was set at a mean excitation energy of 36.4 MeV and beam dose of 2.1×10^{19}. A cross-section limit of 0.56 pb was set in the ^{248}Cm + ^{54}Cr reaction at the SHIP in 2011 [86].

Two experiments with ^{50}Ti beam and target nuclei ^{249}Cf and ^{249}Bk were performed at the TASCA in 2011 and 2012. These were aimed at the synthesis of elements 120 and 119, respectively [87] (The results have not yet been published).

5. Discussion

5.1. Production cross sections

The excitation functions $\sigma_{xn}(E^*)$ of the reactions leading to production of isotopes of elements 112–118 shown in figures 7 and 9 are typical for the process of de-excitation of CN via evaporation of neutrons. The maximum cross-section values correspond to evaporation of three to four neutrons depending on neutron excess in the CN. In comparison with these reaction channels, the evaporation of two neutrons observed in the reactions with ^{242}Pu, ^{243}Am and ^{245}Cm is suppressed by shift of maximum of cross section σ_{2n} below the Coulomb barrier ($E^* < E_{min}$). One should note that different orientations of the deformed target nucleus at the touching point with spherical nucleus ^{48}Ca change location and shape of the Coulomb barrier with regard to the Bass barrier calculated for spherical nuclei. As it follows from measured cross sections $\sigma_{xn}(E^*)$ at the lowest excitation energies E^*, in the reactions Act + ^{48}Ca the CN is formed mainly in 'equatorial' collisions, characterized by minimum distances between the centers of the interacting nuclei, which leads to shift of the cross-section maxima by several MeV to higher values than the corresponding Bass barriers (see figures 7, 9 [56–59]).

With movement of the Coulomb barrier to higher energies $E^* > 50$ MeV, one can expect a decrease of $\sigma_{xn}(E^*)$ because of ascending competition from fission of CN. Indeed, in the reactions of ^{48}Ca with ^{244}Pu and ^{242}Pu at $E^* = 53$ and 50 MeV, respectively (see figure 7), the only single decay chains of ^{287}Fl and ^{285}Fl, products of the 5n-evaporation channel, could be observed. Thus, all the ERs in the Act + ^{48}Ca reactions were registered within relatively narrow excitation-energy interval $29 \le E^* \le 53$ MeV.

In this energy range, the total fusion-evaporation cross sections $\sigma_{tot} = \sum_x \sigma_{xn}(E^*)$ reach maxima at $E^* \approx 40$ MeV (hot fusion); transition of nucleus to the ground state occurs via evaporation of 3–4 neutrons. This energy is about three times larger than excitation energy of nuclei at the cross-section maxima in the cold-fusion reactions used for the synthesis of elements 110–113. The maximum total ER cross sections measured in the experiments on the synthesis of elements with $Z \ge 102$ in cold fusion and in ^{48}Ca-induced reactions are shown in figure 10.

In cold-fusion reactions, as it follows from the figure 10(a), the production cross section drops by about 8 orders of magnitude when Z_{CN} increases from 102 to 113. Such an effect, as a result of growth of the Coulomb factor $k = Z_1 \cdot Z_2 / (A_1^{1/3} + A_2^{1/3})$ by 44% (figure 10(c)), is associated with potential energy surface of the colliding system which causes the hindrance of the formation of CN with stronger Coulomb interaction.

One can note that in theory, the dynamics of the CN formation in competition with the quasi-fission process is the most vague reaction stage. For calculation of the probability P_{fus}, different models are used which suppose different mechanisms of CN formation. In the multidimensional Langevin-type dynamical approach [56–59, 79], it is assumed that two touching nuclei lose their 'individualities' at the touching point and one strongly deformed heavy nucleus with summary mass evaluates in the multidimensional space of deformations

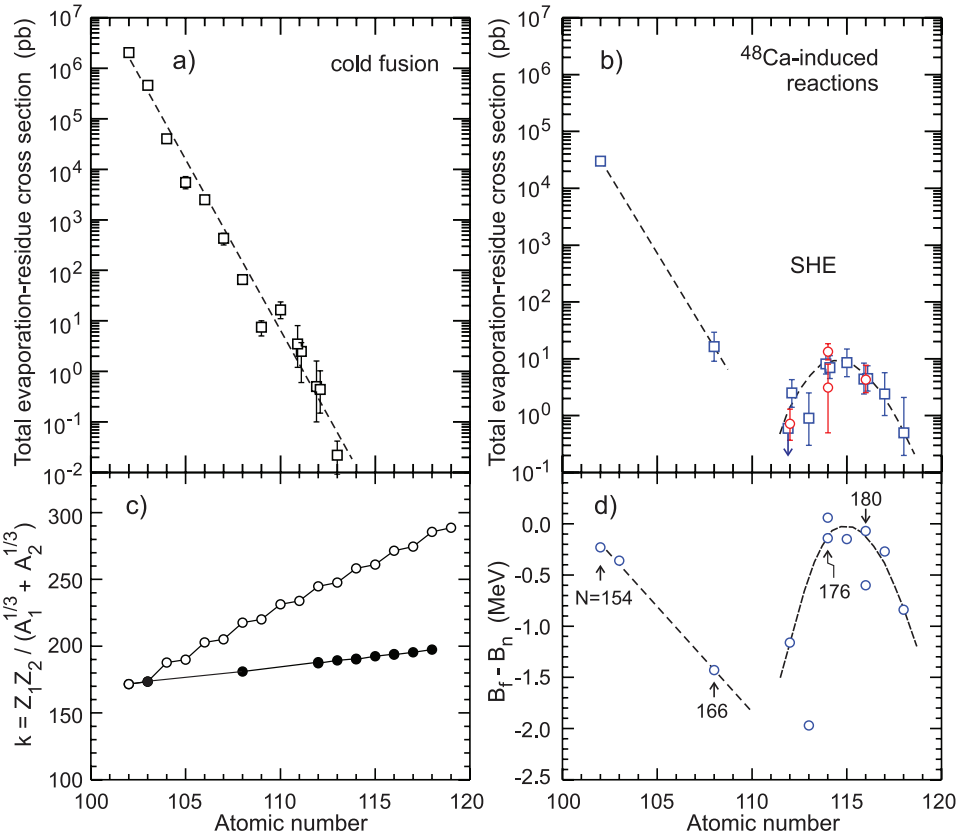

Figure 10. Maximum cross sections of the production of the isotopes of the heavy elements in (*a*) cold fusion reactions: ^{208}Pb, ^{209}Bi + ^{48}Ca, ^{50}Ti, ^{54}Cr, ...^{70}Zn (E^* = 12–20 MeV) and (*b*) hot fusion reactions: ^{208}Pb, ^{226}Ra, ^{233,238}U, ^{242,244}Pu, ^{243}Am, ^{245,248}Cm, ^{249}Bk and ^{249}Cf + ^{48}Ca (E^* = 35–40 MeV) (data from DGFRS and other separators are in blue and red, respectively). In plot (*c*), Coulomb factors $Z_1 \cdot Z_2 / (A_1^{1/3} + A_2^{1/3})$ for nuclei in the cold (open circle) and ^{48}Ca-induced (closed circle) reactions are shown. (*d*) Difference of fission barrier heights (involving non-axial shapes) and neutron binding energies of the CN in ^{48}Ca-induced reactions calculated in macroscopic–microscopic nuclear model [88–90] and corrected for the odd-even effect are shown. Arrows show number of neutrons in the CN with the given atomic number.

into a spherical CN or goes into fission channels. A somewhat different scenario of this process is assumed in the 'dinuclear system model' [81, 82]. The dinuclear system stays in contact configuration and undergoes successive transfer of all nucleons from the lighter nucleus to the heavier partner in competition with the quasi-fission processes. Here two touching nuclei keep their relative distance and their 'individuality'. In still another approach, the extended versions of the 'fusion-by-diffusion' model [61, 83], the stochastic process of shape fluctuations leads to the overcoming of the saddle point. Several analytical formulas for description of the fusion probability are proposed [59, 62, 80]. This reaction stage plays a decisive role in cold-fusion reaction.

On the contrary, in more asymmetric reactions of ^{48}Ca with actinide nuclei the Coulomb repulsion is less. For super-heavy nuclei with Z = 112–118 the Coulomb factor changes by 6.5% only. Because the initial states of the CN Z_{CN} = 112–118 are similar, this allows a uniform description of their transition to ground state via emission of neutrons and γ-rays. The calculated survivability of the CN, which depends on the thermodynamic characteristics of the heated nuclei in the course of their cooling down via emission of neutron(s) and on fission barriers, should correlate with ER cross sections as obtained in the experiment.

In figure 10(*b*), the total cross section $\sigma_{tot} = \sum_x \sigma_{xn}(E^*)$ measured in the experiments in all the reactions of fusion of ^{48}Ca with the target nuclei of Pb, Ra and actinide targets U-Cf are shown. The calculated values of (B_f–B_n) are shown in figure 10(*d*).

Comparing these, one can see that the relatively high cross sections for production of ERs in hot fusion reactions with ^{48}Ca are connected with high survivability of the heated CN. This provides direct evidence of the presence of the high fission barriers in nuclei with Z < 120 which appears due to nuclear shell effects.

5.2. Decay properties

5.2.1. Alpha decay. The energies of α particles for even-Z nuclei ^{281}Cn, ^{294}118, ^{291}Lv, ^{292}Lv, ^{293}Lv and their descendants registered by the focal-plane detector only or together with the side one at the DGFRS [39–45] are shown in figure 11. Here we also show results of experiments carried out with the use of other facilities (see figure 6): chemical setup IVO + COLD [46–49] and separators SHIP [50, 51], BGS [52, 53] and TASCA [32, 54].

In agreement with expectations, the α decays of the even–even nuclei ^{294}118, ^{290,292}Lv and ^{286,288}Fl are terminated by SF

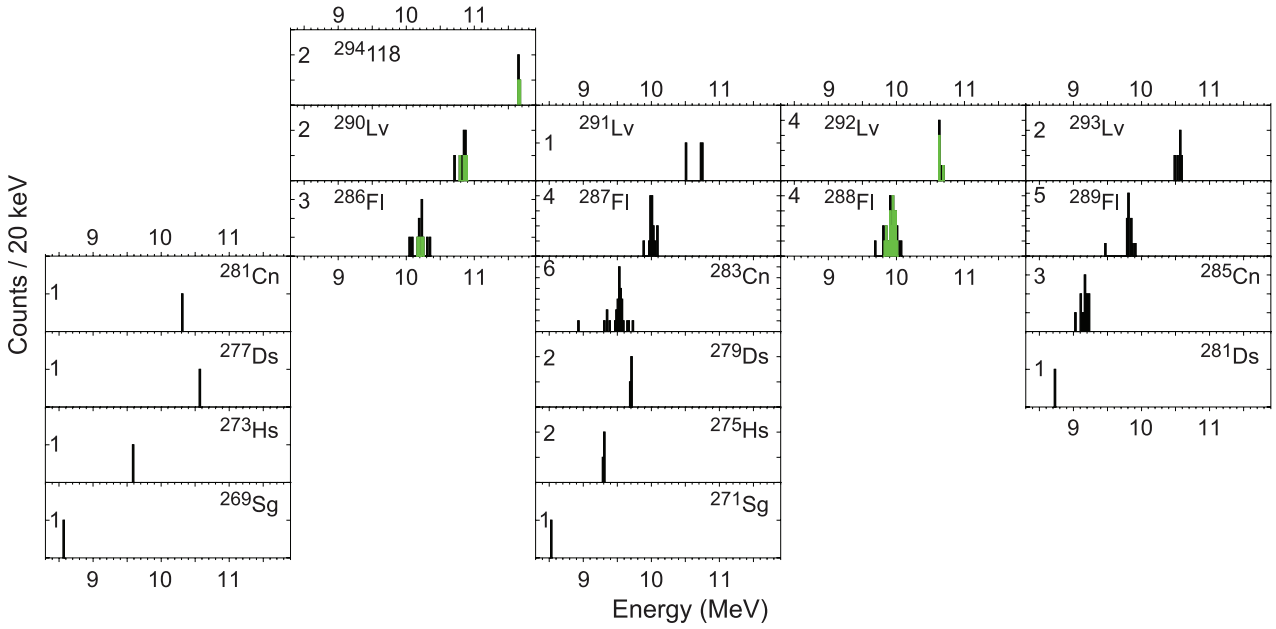

Figure 11. α-particle energy spectra for even-Z nuclei registered by the focal-plane detector only or together with the side one at the DGFRS [39–45], IVO + COLD [46–49], SHIP [50, 51], BGS [52, 53] and TASCA [32, 54]. Note, the energy resolution of α particles ΔE_α detected simultaneously by the focal-plane and side detectors was up to 0.2 MeV (spectra for the events with energy resolution better than 0.1 MeV shown in green). The data from the IVO + COLD are included if ΔE_α are published.

of short-lived isotopes ^{282,284}Cn (see figures 6, 11). The isotope ^{286}Fl has an SF branch of 40^{+11}_{-10} % (68% confidence level). The α-particle energy spectra of these nuclei are characterized mainly by one α line, which corresponds to the ground-state to ground-state transitions as the most probable for even–even nuclei. In figure 11 the spectra of events registered solely by the focal-plane detectors with energy resolution better than 0.1 MeV are shown by green histograms.

The decay chains originated from the even–odd nuclei ^{291,293}Lv are terminated mainly at later stage, by SF of ^{279,281}Ds which have small α-decay branch of 11^{+6}_{-4} % and 7^{+9}_{-5} %, respectively. Two SF events of four observed in the ^{238}U + ^{48}Ca reaction at the SHIP [50] were assigned to 50% SF branch of ^{283}Cn that seemingly does not contradict results observed at the DGFRS in the same reaction [44]. Here, the three decay chains of seven were detected as ER-SF sequences with presumably missing α particles of ^{283}Cn. However, when ^{283}Cn is produced after α decay of the parent nucleus ^{287}Fl [42–45, 52], only the upper limit of 7% for the SF branch of ^{283}Cn can be derived. It seems that the population of isomeric and ground states, even with comparable lifetimes, in direct reaction and after α decay cannot be excluded (compare with ^{261}Rf ([91] and references therein). Further α decay of the even–odd nuclei leads to SF of ^{265,267}Rf and ^{277}Hs (SF branch for ^{271}Sg is not excluded with probability of 40%).

The α-particle energy spectra of the even–odd isotopes are broader. The complex spectra are clearly seen for ^{283}Cn, ^{289}Fl and ^{291}Lv. In addition to the main α line at E_α = 9.53 MeV, two lines with lower energies of 9.33 and 8.94 MeV were registered for ^{283}Cn [42–47] whereas a spectrum of ^{287}Fl is consistent with a single α transition. The hindrance factors (HF) of $1.5^{+0.5}_{-0.3}$, $0.3^{+1.5}_{-0.14}$ and $2.9^{+1.7}_{-1.6}$, respectively, for three energies of ^{283}Cn can be estimated as a ratio of partial half-lives which are determined by numbers of observed events and half-lives expected for Z = 112 nucleus with measured α-particle energies from, e.g. semi-empirical systematics (Viola–Seaborg formula [92]). Such data could be decisive for predictions of the low-lying quasi-particle states of nuclei. Predominantly single-line spectrum is seen for ^{293}Lv but two different energies were observed for ^{289}Fl with E_α = 9.48 and 9.84 MeV. Both these α decays are unhindered (HF = $1.1^{+0.6}_{-0.8}$ and $1.1^{+0.5}_{-0.2}$, respectively).

The energy spectra of α particles for odd-Z nuclei ^{282}113, ^{287,288}115, ^{293,294}117 and their descendants registered at the DGFRS [26, 27, 34, 36, 66–70] and TASCA [73, 74] are shown in figure 12. Even in cases with relatively low statistics, one can see wider energy distributions for these nuclei than those shown in figure 11. The α-decay chains of four parent nuclei end by SF of isotopes ^{266,267,268,270}Db. Only odd–even ^{281}Rg undergoes SF with small branch for α decay ($b_\alpha = 12^{+9}_{-7}$ %) which is followed by SF of ^{277}Mt (see figure 8).

The decay properties of nuclei produced in the fusion-evaporation reactions with ^{48}Ca are shown in figures 6 and 8 and table 1. The α-decay energies of nuclei $Q_\alpha^{\rm th}$ calculated within macroscopic–microscopic model [88, 89] are given in column 9. For even–even nuclei with Z = 114–118 and N = 172–176 the values $\Delta Q_\alpha = Q_\alpha^{\rm exp} - Q_\alpha^{\rm th}$ amount to from −0.5 to −0.1 MeV. Measured in experiments α-decay energies $Q_\alpha^{\rm exp}$ are lower and correspondingly, the half-lives $T_\alpha^{\rm exp}$ of superheavy nuclei are larger than theoretical values. For even-Z isotopes of elements 106–116 with odd number of neutrons N = 165–177 the difference ΔQ_α varies within −0.8–0.4 MeV. Finally, for odd-Z nuclei of elements 107–117 the discrepancies are ΔQ_α = −1.1–0.4 MeV in assumption that the measured maximum α-particle energy corresponds to transitions through the ground states of odd-Z nuclei which is not always

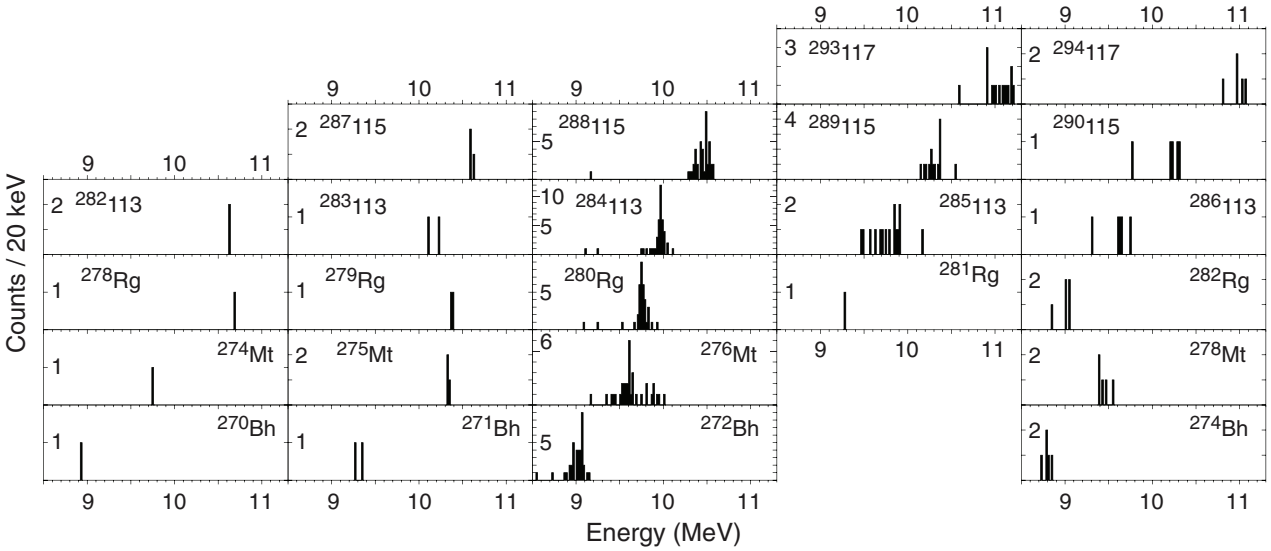

Figure 12. α-particle energy spectra for odd-Z nuclei registered by the focal-plane detector only or together with the side one at the DGFRS [26, 27, 34, 36, 66–70] and TASCA [73, 74].

valid. From comparison of decay properties of 43 α-decaying nuclei produced in the Act + ^{48}Ca reactions, it follows that their agreement with theoretical predictions is not only qualitative but, to some extent, quantitative. Here one should bear in mind that accuracy of predictions of masses of the known nuclei reaches 0.3–0.4 MeV [89] and 0.4–0.7 MeV for some other approaches (see, e.g. review [22] and references therein). Note, results of Q_α^{th} calculations within other MM models and purely microscopic approaches (HFB, RMF) also agree with experimental data ([22] and references therein). Therefore, the hypothesis of existence of super-heavy nuclei received experimental confirmation.

5.2.2. Spontaneous fission. For 16 of the 54 synthesized nuclei SF was observed. For seven even-Z nuclei SF is the predominant mode of decay (see figure 6 and table 1). In five nuclei, SF competes with α decay. As to the odd-Z nuclei, SF was registered for six nuclides (figure 8 and table 1). For the remaining nuclides SF was not observed. The partial SF half-lives of even–even isotopes with $N \geq 162$, produced in fusion reactions with ^{48}Ca, together with the half-lives of SF nuclides with $N < 162$, are shown in figure 13. Two isotopes of element 112 with N = 170 and 172 are located in a region, where a steep rise of $T_{\text{SF}}(N)$ is expected. Indeed, in the even–even isotopes ^{282}Cn and ^{284}Cn the difference in two neutrons increases the partial half-life T_{SF} by two orders of magnitude[4]. A similar effect is also observed for the even–even isotopes of element 114. Addition of two neutrons to the nucleus ^{286}Fl ($T_{\text{SF}} \approx 0.3$ s) leads to increase of the stability of ^{288}Fl with respect to SF by at least a factor of 15. For even–even isotopes ^{288}Fl, ^{290}Lv, ^{292}Lv and ^{294}118 SF was not observed.

It is significant that the rise of stability with respect to SF is observed for the heavy nuclei with $Z \geq 110$, which are 10–12 neutrons farther from the closed neutron shell N = 184. On

[4] From measured SF half-lives of the even–even isotopes ^{282}Cn and ^{284}Cn it follows that the odd neutron in the ^{283}Cn nucleus imposes a hindrance to spontaneous fission exceeding 5000.

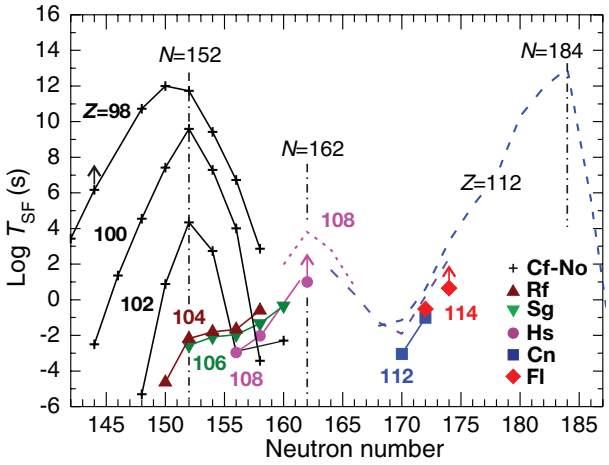

Figure 13. Common logarithm of partial spontaneous fission half-life versus. neutron number for even–even isotopes of elements with Z = 98–114 [32, 42–45, 49, 51–54, 93]. Dashed lines show the theoretical T_{SF} values [7, 8] for even–even Z = 108 (in magenta), 110 (in violet) and 112 (in blue) isotopes.

moving to the nuclei with $Z < 110$ and $N < 170$ the probability of SF decreases again when the closed deformed shell N = 162 is approached. The stabilizing effect of the N = 162 shell manifests itself in the properties of the even–even isotopes of Rf, Sg and Hs.

Because of the high hindrance of SF in the nuclei with odd number of protons (and neutrons) and relatively low T_α, the isotopes of elements 113 and 115 produced in the reactions ^{237}Np + ^{48}Ca and ^{243}Am + ^{48}Ca with N = 169–173 undergo α decay [26, 27, 34, 36, 66–70, 73]. Spontaneous fission is observed only at the end of chain for isotopes of element 105 (or their EC/α-decay products). For ^{268}Db α decay seems to be less probable (see above).

In case of the reaction ^{249}Bk(^{48}Ca,3-4n)^{294,293}117, the daughter nuclei have one or two extra neutrons compared to the reaction with ^{243}Am. In analogy with the neighbouring even-Z isotopes all the nuclei in the decay chains of ^{293}117

and ^{294}117 with $Z > 111$ and $N \geq 172$ will undergo α decay. The nucleus ^{281}Rg ($N = 170$) belonging to the 'critical' region between neutron shells $N = 162$ and 184 might avoid SF due to the hindrance resulting from an odd proton. The hindrance of the SF in ^{281}Rg with respect to its even–even neighbuor ^{282}Cn [42–45, 52, 53] is ~ 2×10^4. Despite this, the isotope ^{281}Rg undergoes SF with a probability of about 90%. Accordingly, even the high hindrance governed by oddness does not 'save' the odd nucleus (^{281}Rg, ^{277}Mt) from SF which is caused by the weakening of the stabilizing effect of the neutron shells at $N = 162$ and $N = 184$. However an extra neutron and the double effect of oddness favor the α decay in the neighboring isotopes ^{280}Rg and ^{282}Rg.

Practically for none of the odd-Z nuclei the branch for EC/β^+ was observed. For example, isotope ^{288}Fl, EC product of ^{288}115 and its descendants were not seen in the ^{243}Am + ^{48}Ca reaction, which indicates that for nuclei in the decay chain of ^{288}115 the probability for EC/β^+ is less than 2%. Meanwhile, nuclei at the end of decay chains, neutron-rich odd–odd isotopes ^{266,268,270}Db, could undergo EC decay leading to SF of even–even Rf isotopes for which $T_{SF} = 23$ s, 1.4 s and 20 ms are predicted [7]. For odd–even isotopes ^{267}Db as well as ^{281}Rg values of the observed half-lives are somewhat lower than the bulk of data in the systematics of T_β versus Q_β for known isotopes of Np-Db (see, e.g. figure 7 in [27]). This could indicate a larger probability of undergoing SF than EC/$_\beta^+$ decay leading to 1 h ^{267}Rf and 13 s ^{281}Ds.

Spontaneously fissioning nuclei with $Z = 108$–112 and $N = 168$–170 located between $N = 162$ and $N = 184$ neutron shells have the lowest T_{SF} values. The α-decay chains of the heaviest nuclei both with even and odd Z, N numbers are terminated here by SF. The decay chains of nuclei outside this region end by SF of neutron-rich isotopes of Rf and Db located closer to the neutron shell at $N = 162$. Thus, the decay chains of the heaviest nuclei synthesized in the Act + ^{48}Ca reactions are not connected with a region of known nuclei. They form an isolated region of the heaviest nuclei—some 'island of superheavy nuclei'. The existence of this island and relatively high stability of SHN are determined in full by the new closed shells at $N = 184$ and $Z = 114$ (possibly 120–126).

Investigation of SF of SHN is of independent interest. Extensive information about the SF process, obtained for nuclei in the region of actinides (especially for ^{252}Cf), can be essentially extended for heavier and super-heavy nuclei whose fission barrier is entirely determined by the influence of the new nuclear shells.

6. Perspectives

For the synthesis of super-heavy nuclei with the largest neutron excess $N = 175$–177, the heavy isotopes ^{244}Pu, ^{248}Cm, ^{249}Bk and ^{249}Cf produced at high flux reactors were used as target nuclei. Experiments aimed at the synthesis of the new isotopes of element 118 in the $^{249–251}$Cf + ^{48}Ca reactions are being considered at FLNR. As a target material, there will be used the long-lived isotopes of Cf extracted from 'old' ^{252}Cf neutron sources which were made 30–40 years ago at the HFIR (ORNL). With such a target of mixed isotopes of californium, in the 3n- and 4n-evaporation channels, the three new isotopes - ^{293}118, ^{295}118 and ^{296}118—could be produced. Note that ^{251}Cf is the heaviest nuclide that can be produced at the HFIR in required amounts. For the synthesis of elements with $Z > 118$, projectiles of heavier than ^{48}Ca have to be used.

Another direction is to recede from the shell at $N = 184$ and investigate SHN with lower neutron excess that could result in connection of region of known nuclei and 'island of SHN'. For these purposes, light isotopes of actinides, such as $^{233–236}$U, ^{239,240}Pu or ^{241}Am, can be used in the reactions with ^{48}Ca which leads to isotopes of $Z = 112$–115 elements with $N = 165$–172. However, deficit of neutrons—shift to the edge of island of stability and withdrawal from the shell at $N = 184$—can result in reduce of production cross sections caused by decrease of fission barriers and correspondingly, survivability of CN. This effect was already revealed in the experiments on the synthesis of light isotopes of elements 112–114 in the ^{233}U, ^{237}Np and ^{239}Pu + ^{48}Ca reactions [44, 68]. Further attempts in this direction, with the existing sensitivity of experiment, does not seem a trivial task. At the same time, discovery of SHN raises many questions concerning the validity of the application of the nuclear shell model and the limits of existence of the heaviest nuclei, about the sizes and nuclear density of the SHN, atomic structure and chemical properties of super-heavy elements. Still an open question is: can the SHN be produced in nucleosynthesis?

Obviously, further investigations of the heaviest nuclei and synthesis of the new elements call for considerable increase in the sensitivity of equipment used in experiments. Our knowledge of the decay properties of SHN and their production cross sections in the ^{48}Ca-induced reactions as well as the latest achievements in accelerator and plasma physics, reactor technologies and experimental techniques form the basis for creation of the new laboratory—type of a factory for continuous production of super-heavy nuclei (SHE Factory). Expected yield of SHN can be increased by almost two orders of magnitude compared with the existing level. Since the beginning of 2013, at FLNR (JINR) the construction of the SHE Factory is under way.

Acknowledgments

It is our pleasure to convey gratitude to all 60 co-authors of the original publications for their hard work and active participation in the experimental programme on the synthesis and study of the properties of super-heavy elements. Presented results from the DGFRS were obtained owing to common efforts of many our colleagues over fifteen years. Not all of them are co-authors of the papers. We are grateful to them for their important contributions.

The investigations reported in this review involve numerous experiments performed in Dubna in 1999–2014. This was preceded by the 5 year work aimed at increase of the ^{48}Ca beam, further development of methods of preparation of actinide targets, modernization of the DGFRS and its detection system for registration of rare events of production and decay of SHN,

etc. The experiments were carried out in collaboration with groups from US National Laboratories in Livermore and Oak Ridge, RIAR in Dimitrovgrad (Russia), Vanderbilt University in Nashville and University of Tennessee in Knoxville (USA), PSI in Villigen (Switzerland), RIEPh in Sarov (Russia). The investigation of SHN is one of the high-priority directions in the scientific programme of the JINR. During all stages of the experiments, we received support from the Committee of Plenipotentiaries of the Governments of the JINR Member States, JINR Directorate and Scientific Council.

These studies were performed with the support of the Russian Ministry of Atomic Energy, of the Governor of the Moscow region and permanently of the Russian Foundation for Basic Research, including recent Grants No. 13-02-12052 and No. 13-03-12205. Research at ORNL was supported by the U S DOE Office of Nuclear Physics under DOE Contract No. DE-AC05-00OR22725 with UTBattelle, LLC. Research at LLNL was supported by LDRD Program Project No. 08-ERD-030, under DOE Contract No. DE-AC52-07NA27344 with Lawrence Livermore National Security, LLC. This work was also supported by the U S DOE through Grant No. DE-FG-05-88ER40407 (Vanderbilt University). These studies were performed in the framework of the Russian Federation/U S Joint Coordinating Committee for Research on Fundamental Properties of Matter.

References

[1] Bohr N and Wheeler J A 1939 The mechanism of nuclear fission *Phys. Rev.* **56** 426–50
[2] Polikanov S M *et al* 1962 Spontaneous fission with an anomalously short period *Sov. Phys. JETF* **15** 1016–21
[3] Singh B, Zywina R and Firestone R 2002 Table of superdeformed nuclear bands and fission isomers *Nucl. Data Sheets* **97** 241–592
[4] Oganessian Y T 2007 Heaviest nuclei from ^{48}Ca-induced reactions *J. Phys. G: Nucl. Part. Phys.* **34** R165–242
[5] Myers W D and Swiatecki W J 1966 Nuclear masses and deformations *Nucl. Phys.* **81** 1–60
[6] Myers W D and Swiatecki W J 1967 Anomalies in nuclear masses *Ark. Fys.* **36** 343–52
[7] Smolańczuk R, Skalski J and Sobiczewski A 1995 Spontaneous-fission half-lives of deformed superheavy nuclei *Phys. Rev.* C **52** 1871–80
[8] Smolańczuk R 1997 Properties of the hypothetical spherical superheavy nuclei *Phys. Rev.* C **56** 812–24
[9] Strutinsky V M 1967 Shell effects in nuclear masses and deformation energies *Nucl. Phys.* A **95** 420–42
[10] Brack M *et al* 1972 Funny hills: The shell-correction approach to nuclear shell effects and its applications to the fission process *Rev. Mod. Phys.* **44** 320–405
[11] Möller P and Nix J R 1994 Stability of heavy and superheavy elements *J. Phys. G: Nucl. Part. Phys.* **20** 1681–747
[12] Greiner W 1996 On the extension of the periodic system into the sectors of strangeness and antimatter *Int. J. Mod. Phys.* E **5** 1–92
[13] Sobiczewski A 1994 Progress in theoretical understanding of properties of heaviest nuclei *Phys. Part. Nucl.* **25** 295–11
[14] Sobiczewski A, Gareev F A and Kalinkin B N 1966 Closed shells for Z ≥ 82 and $N \geq 126$ in a diffuse potential well *Phys. Lett.* **22** 500–2
[15] Meldner H 1967 Predictions of new magic regions and masses for super-heavy nuclei from calculations with realistic shell model single particle Hamiltonians *Ark. Fys.* **36** 593–8
[16] Nilsson S G *et al* 1968 On the spontaneous fission of nuclei with Z near 114 and N near 184 *Nucl. Phys.* A **115** 545–62
[17] Mosel U and Greiner W 1969 On the stability of superheavy nuclei against fission *Z. Phys.* **222** 261–82
[18] Patyk Z and Sobiczewski A 1991 Ground-state properties of the heaviest nuclei analyzed in a multidimentional deformation space *Nucl. Phys.* A **533** 132–52
[19] Patyk Z and Sobiczewski A 1991 Main deformed shells of heavy nuclei studied in a multidimensional deformation space *Phys. Lett.* B **256** 307–10
[20] Hofmann S and Münzenberg G 2000 The discovery of the heaviest elements *Rev. Mod. Phys.* **72** 733–67
[21] Hofmann S 2009 Superheavy elements *Lect. Notes Phys.* **764** 203–52
[22] Sobiczewski A and Pomorski K 2007 Description of structure and properties of superheavy nuclei *Prog. Part. Nucl. Phys.* **58** 292–49
[23] Oganessian Y T *et al* 1975 Experiments on the synthesis of neutron-deficient kurchatovium isotopes in reaction induced by ^{50}Ti ions *Nucl. Phys.* A **239** 157–71
[24] Subotic K *et al* 2002 Evaporation residue collection efficiencies and position spectra of the Dubna gas-filled recoil separator *Nucl. Instrum. Methods Phys. Res.* A **481** 71–80
[25] Oganessian Y T *et al* 2001 Average charge states of heavy atoms in dilute hydrogen *Phys. Rev.* C **64** 064309
[26] Oganessian Y T *et al* 2005 Synthesis of elements 115 and 113 in the reaction ^{243}Am + ^{48}Ca *Phys. Rev.* C **72** 034611
[27] Oganessian Y T *et al* 2011 Eleven new heaviest isotopes of elements $Z = 105$ to $Z = 117$ identified among the products of ^{249}Bk + ^{48}Ca reactions *Phys. Rev.* C **83** 054315
[28] Oganessian Y T 1991 Gas filled separator of recoil nuclei *Heavy Ion Physics JINR LNR Scientific Report* 1989–1990 p 158–9 (Dubna)
[29] Gregorich K E 2013 Simulation of recoil trajectories in gas-filled magnetic separators *Nucl. Instrum. Methods Phys. Res.* A **711** 47–59
[30] Ninov V, Gregorich K E and McGrath C A 1998 The Berkeley gas-filled separator *AIP Conf. Proc.* **455** 704–7
[31] Semchenkov A *et al* 2008 The transactinide separator and chemistry apparatus (TASCA) at GSI—Optimization of ion-optical structures and magnet designs *Nucl. Instrum. Methods Phys. Res.* B **266** 4153–61
[32] Gates J M *et al* 2011 First superheavy element experiments at the GSI recoil separator TASCA: The production and decay of element 114 in the ^{244}Pu(^{48}Ca, 3-4n) reaction *Phys. Rev.* C **83** 054618
[33] Sagaidak R N, Utyonkov V K and Scarlassara F 2013 Simulation of angular and energy distributions for heavy evaporation residues using statistical model approximations and TRIM code *Nucl. Instrum. Methods Phys. Res.* A **700** 111–23
[34] Oganessian Y T *et al* 2013 Experimental studies of the ^{249}Bk + ^{48}Ca reaction including decay properties and excitation function for isotopes of element 117 and discovery of the new isotope ^{277}Mt *Phys. Rev.* C **87** 054621
[35] Tsyganov Yu S *et al* 2004 Detection system for heavy element research: present status *Nucl. Instrum. Methods Phys. Res.* A **525** 213–6
[36] Oganessian Y T *et al* 2012 Production and decay of the heaviest nuclei $^{293,\,294}$117 and ^{294}118 *Phys. Rev. Lett.* **109** 162501
[37] Barber R C *et al* 1992 Discovery of the transfermium elements *Prog. Part. Nucl. Phys.* **29** 453–530
[38] Hoffman D C and Lane M R 1994 Spontaneous fission *Radiochim. Acta* **70/71** 135–45

[39] Oganessian Y T *et al* 2000 Synthesis of superheavy nuclei in the ^{48}Ca + ^{244}Pu reaction: ^{288}114 *Phys. Rev.* C **62** 041604 (R)

[40] Oganessian Y T *et al* 2000 Observation of the decay of ^{292}116 *Phys. Rev.* C **63** 011301(R)

[41] Oganessian Y T, Utyonkov V K and Moody K J 2001 Synthesis of ^{292}116 in the ^{248}Cm + ^{48}Ca reaction *Phys. At. Nucl.* **64** 1349–55

[42] Oganessian Y T *et al* 2004 Measurements of cross sections for the fusion-evaporation reactions ^{244}Pu(^{48}Ca, xn)$^{292-x}$114 and ^{245}Cm(^{48}Ca, xn)$^{293-x}$ 116 *Phys. Rev.* C **69** 054607

[43] Oganessian Y T *et al* 2004 Measurements of cross sections and decay properties of the isotopes of elements 112, 114 and 116 produced in the fusion reactions $^{233,\,238}$U, ^{242}Pu and ^{248}Cm + ^{48}Ca Preprint JINR E7-2004–160 www.info.jinr.ru/publish/Preprints/2004/160(E7-2004–160).pdf

[44] Oganessian Y T *et al* 2004 Measurements of cross sections and decay properties of the isotopes of elements 112, 114 and 116 produced in the fusion reactions $^{233,\,238}$U, ^{242}Pu and ^{248}Cm + ^{48}Ca *Phys. Rev.* C **70** 064609

[45] Oganessian Y T *et al* 2006 Synthesis of the isotopes of elements 118 and 116 in the ^{249}Cf and ^{245}Cm + ^{48}Ca fusion reactions *Phys. Rev.* C **74** 044602

[46] Eichler R *et al* 2007 Chemical characterization of element 112 *Nature* **447** 72–5

[47] Eichler R *et al* 2008 Thermochemical and physical properties of element 112 *Angew. Chem. Int. Edn* **47** 3262–6

[48] Wittwer D *et al* 2010 Gas phase chemical studies of superheavy elements using the Dubna gas-filled recoil separator—Stopping range determination *Nucl. Instrum. Methods Phys. Res.* B **268** 28–35

[49] Eichler R *et al* 2010 Indication for a volatile element 114 *Radoichim. Acta* **98** 133–9

[50] Hofmann S *et al* 2007 The reaction ^{48}Ca + ^{238}U → ^{286}112* studied at the GSI-SHIP *Eur. Phys. J.* A **32** 251–60

[51] Hofmann S *et al* 2012 The reaction ^{48}Ca + ^{248}Cm → ^{296}116* studied at the GSI-SHIP *Eur. Phys. J.* A **48** 62 and private communication

[52] Stavsetra L *et al* 2009 Independent verification of element 114 production in the ^{48}Ca + ^{242}Pu reaction *Phys. Rev. Lett.* **103** 132502

[53] Ellison P A *et al* 2010 New superheavy element isotopes: ^{242}Pu(^{48}Ca, 5*n*)^{285}114 *Phys. Rev. Lett.* **105** 182701

[54] Düllmann Ch E *et al* 2010 Production and decay of element 114: high cross sections and the new nucleus ^{277}Hs *Phys. Rev. Lett.* **104** 252701

[55] Bass R 1980 Fusion reactions: successes and limitations of a 1D description *Proc. Symp. Deep Inelastic and Fusion Reactions with Heavy Ions (Berlin, 23–25 October 1979)* vol 117 ed W von Oertzen *Lecture Notes in Physics* (Berlin: Springer-Verlag) p 281–93

[56] Zagrebaev V I *et al* 2001 Synthesis of superheavy nuclei: How accurately can we describe it and calculate the cross sections? *Phys. Rev.* C **65** 014607

[57] Zagrebaev V I, Itkis M G and Oganessian Y T 2003 Fusion–fission dynamics and perspectives of future experiments *Phys. At. Nucl.* **66** 1033–41

[58] Zagrebaev V I 2004 Fusion–fission dynamics of super-heavy element formation and decay *Nucl. Phys.* A **734** 164–7

[59] Zagrebaev V and Greiner W 2008 Synthesis of superheavy nuclei: A search for new production reactions *Phys. Rev.* C **78** 034610

[60] Schmidt K-H, Sahm C-C, Pielenz K and Clerc H-G 1984 Some remarks on the error analysis in the case of poor statistics *Z. Phys.* A **316** 19–26

[61] Siwek-Wilczyńska K *et al* 2012 Predictions of the fusion-by-diffusion model for the synthesis cross sections of $Z = 114$–120 elements based on macroscopic-microscopic fission barriers *Phys. Rev.* C **86** 014611

[62] Zhang J J, Wang C B and Ren Z Z 2013 Calculation of evaporation residue cross sections for the synthesis of superheavy nuclei in hot fusion reactions *Nucl. Phys.* A **909** 36–49

[63] Barber R C *et al* 2011 Discovery of the elements with atomic numbers greater than or equal to 113 (IUPAC Technical Report) *Pure Appl. Chem.* **83** 1485–98, Errata: Barber R C *et al* 2011 *Pure Appl. Chem.* **83** 1801

[64] Loss R D and Corish J 2012 Names and symbols of the elements with atomic numbers 114 and 116 (IUPAC Recommendations 2012) *Pure Appl. Chem.* **84** 1669–72

[65] Yakushev A *et al* 2014 Superheavy element flerovium (element 114) is a volatile metal *Inorg. Chem.* **53** 1624–9

[66] Oganessian Y T *et al* 2013 Investigation of the ^{243}Am + ^{48}Ca reaction products previously observed in the experiments on elements 113, 115 and 117 *Phys. Rev.* C **87** 014302

[67] Oganessian Y T *et al* 2004 Experiments on the synthesis of element 115 in the reaction ^{243}Am(^{48}Ca, xn)$^{291-x}$115 *Phys. Rev.* C **69** 021601(R)

[68] Oganessian Y T *et al* 2007 Synthesis of the isotope ^{282}113 in the ^{237}Np + ^{48}Ca fusion reaction *Phys. Rev.* C **76** 011601(R)

[69] Oganessian Y T *et al* 2010 Synthesis of a new element with atomic number $Z = 117$ *Phys. Rev. Lett.* **104** 142502

[70] Oganessian Y T *et al* 2012 New insights into the ^{243}Am + ^{48}Ca reaction products previously observed in the experiments on elements 113, 115 and 117 *Phys. Rev. Lett.* **108** 022502

[71] Dmitriev S N *et al* 2005 Chemical identification of dubnium as a decay product of element 115 produced in the reaction ^{48}Ca + ^{243} *Am. Mendeleev Commun.* **15** 1

[72] Stoyer N J *et al* 2007 Chemical identification of a long-lived isotope of dubnium, a descendant of element 115 *Nucl. Phys.* A **787** 388c–95c

[73] Rudolph D *et al* 2013 Spectroscopy of element 115 decay chains *Phys. Rev. Lett.* **111** 112502

[74] Khuyagbaatar J *et al* 2014 ^{48}Ca + ^{249}Bk Fusion reaction leading to element $Z = 117$: Long-lived α-decaying ^{270}Db and discovery of ^{266}Lr *Phys. Rev. Lett.* **112** 172501

[75] Schumann D *et al* 2005 Chemical procedure applied for the identification of Rf/Db produced in the ^{48}Ca + ^{243}Am reaction *Radiochim. Acta* **93** 727–32

[76] Zlokazov V B 1978 Program for constructing the estimates of the parameter of the exponential distribution under conditions of poor statistics *Nucl. Instrum. Methods* **151** 303–6

[77] Carlson T A and Nestor C W Jr 1977 Calculation of K and L x rays for elements of $Z = 95$ to 130 *At. Data Nucl. Data Tables* **19** 153–73

[78] Wang M *et al* 2012 The AME2012 atomic mass evaluation *Chin. Phys.* C **36** 1603–2014

[79] Zagrebaev V I, Karpov A and Griener W 2014 Synthesis of superheavy nuclei: nearest and distant opportunities *Acta Phys. Pol.* B **45** 291–302

[80] Wang N, Tian J and Scheid W 2011 Systematics of fusion probability in 'hot' fusion reactions *Phys. Rev.* C **84** 061601(R)

[81] Nasirov A K *et al* 2011 Effects of the entrance channel and fission barrier in the synthesis of superheavy element $Z = 120$ *Phys. Rev.* C **84** 044612

[82] Kuzmina A N, Adamian G G, Antonenko N V and Scheid W 2012 Influence of proton shell closure on production and identification of new superheavy nuclei *Phys. Rev.* C **85** 014319

[83] Liu Z H and Bao J D 2013 Possibility to produce element 120 in the ^{54}Cr + ^{248}Cm hot fusion reaction *Phys. Rev.* C **87** 034616

[84] Oganessian Y T *et al* 2009 Attempt to produce element 120 in the ^{244}Pu + ^{58}Fe reaction *Phys. Rev.* C **79** 024603

[85] Hofmann S *et al* 2009 Probing shell effects at $Z = 120$ and $N = 184$ *GSI Scientific Report 2008*, *GSI Report* 2009-1 131

[86] Hofmann S *et al* 2012 Attempts for the synthesis of new elements at SHIP *GSI Scientific Report 2011*, *GSI Report* 2012-1 205
[87] Düllmann Ch E *et al* 2012 Upgrade of the gas-filled recoil separator TASCA and first search experiment for the new element 120 in the reaction ^{50}Ti + ^{249}Cf *GSI Scientific Report 2011*, *GSI Report* 2012-1 206
[88] Muntian I, Hofmann S, Patyk Z and Sobiczewski A 2003 Properties of heaviest nuclei *Acta Phys. Pol.* B **34** 2073–82
[89] Muntian I, Patyk Z and Sobiczewski A 2003 Calculated masses of heaviest nuclei *Phys. At. Nucl.* **66** 1015–9
[90] Kowal M, Jachimowicz P and Sobiczewski A 2010 Fission barriers for even–even superheavy nuclei *Phys. Rev.* C **82** 014303 and private communication
[91] Haba H *et al* 2011 Production and decay properties of the 1.9-s isomer state in ^{261}Rf *Phys. Rev.* C **83** 034602
[92] Viola V E Jr and Seaborg G T 1966 Nuclear systematics of the heavy elements—II. Lifetimes for alpha, beta and spontaneous fission decay *J. Inorg. Nucl. Chem.* **28** 741–61
[93] Audi G *et al* 2012 The NUBASE2012 evaluation of nuclear properties *Chin. Phys.* C **36** 1157–286